

# M.E.M.S FOR EXTRACTING USABLE ELECTRICAL POWER FROM QUANTUM VACUUM ENERGY WHILE REMAINING COMPLIANT WITH EMMY NOETHER'S THEOREM

Sangouard Patrick

ESIEE Paris, France

## ABSTRACT

*We know that the absolutely nothing, the total energy vacuum, does not exist. We have known this for a long time theoretically, but more recently thanks to many experiments that have proven it.*

***"Nothing" does not exist, so the void is far from being "nothing".***

*The quantum vacuum that permeates our universe contains, within the smallest volume of space, and within the bounds of Heisenberg's uncertainty principle, a multitude of radiation and virtual particles along with their antiparticles constantly created and annihilated. These particles are called virtual because their lifetime is extremely short ( $10^{-22}$  seconds for an electron with its positron). The quantum vacuum is filled with energy. This observation comes from HEISENBERG'S inequalities stipulating that  $\Delta E \cdot \Delta t \geq \hbar / 2$ . With  $\Delta E$  = energy variation  $\Delta t$  = time duration of this variation,  $\hbar$  is the reduced Planck constant. It is possible theoretically to borrow energy from the vacuum for a very short time.*

*This statement has been proven many times and observed by undeniable physical effects, for example :*

- *The Lamb shift (1947) of atomic emission frequencies:*
- *By the Van der Waals force which plays a very important physicochemical role and had a quantum interpretation in 1930 [London]*
- *By Hawking's radiation theory, predicted in 1974 and observed on 7 September 2016.*
- *And in particular by the experimental verification (in 1958 but especially in 1997) of the existence of a so-called Casimir force between two very close plates. Mr. Casimir first formulated this force into an equation in 1948, which Mr. Lifshitz E.M. improved in 1956 to include non-zero temperature  $T$ .*

## 1. OBTAINING AN ELECTRIC CURRENT FROM VACUUM

For the rest of this presentation, we will use a reference frame consisting of our 4-dimensional space-time continuum augmented with the unknown dimensions of the quantum vacuum. This choice makes it possible to explain that the apparent "perpetual motion" of the M.E.M.S. (Micro Electro Mechanical System) device presented makes it possible to obtain exploitable electrical power, at the output of autonomous electronics which does not come, of course, from 'nothing' but from the perpetual and universal supply of energy of the ocean of quantum vacuum.

However, the problem is not so much to extract energy from the vacuum as to extract it without spending more energy than one can hope to recover. **This extraction must be in accordance with the theorem (1915) of the mathematician EMMY NOETHER.**

We use in our MEMS the attractive Casimir force  $F_{CA} = S_S \frac{\pi^2 c \hbar}{240 z_s^4}$  .Eq 1 .

With  $S_S$  the surface of Casimir's electrodes ,  $\hbar = h/2\pi$  the reduce Planck constant,  $c$  the speed of light,  $z_s$  the interface of Casimir's electrodes .

We notice that this variation of  $F_{CA}$  in  $1/z_s^4$ , would imply that a larger opposing force is provided to return to the initial position with the decrease in the interface of Casimir's electrodes  $z_s$ .

Coulomb's force can play this role and with an energy balance satisfying Emmy Noether's theorem, because this force will be in  $1/z_s^{10}$ .

The vibrating part of the MEMS is showing figure 1

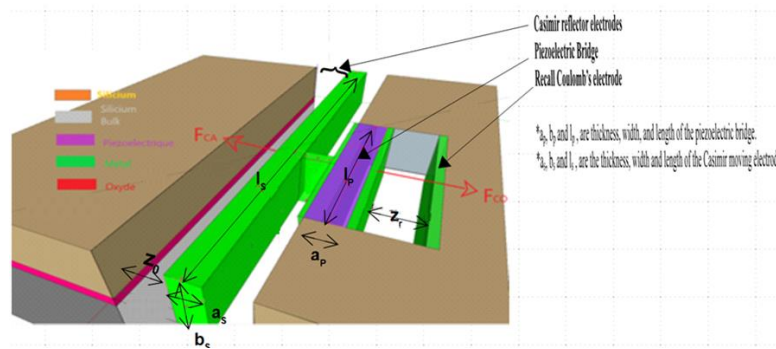
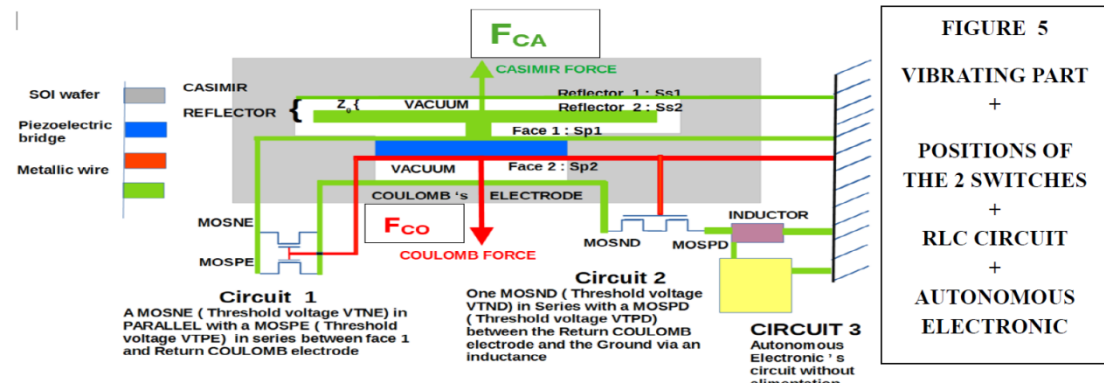


FIGURE 1 Vue of the vibrating part of the MEMS

In fact, we know that fixed charges  $Q_F$  are induced in a piezoelectric bridge during a deformation produced by a force . When this deformation is perpendicular to the polarization of a piezoelectric film, they are then proportional to this force , here the Casimir force  $F_{CA}$  , and follow the law  $Q_F = \frac{d_{31} l_p}{a_p} F_{CA} \Rightarrow Q_F = \frac{d_{31} l_p}{a_p} S \frac{\pi^2 c \hbar}{240} \left( \frac{1}{z_s^4} - \frac{1}{z_0^4} \right)$  Eq 2

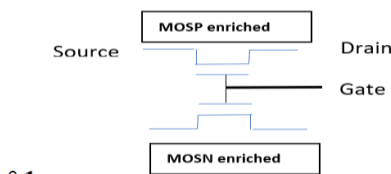
In this expression  $z_0$ = the initial position without any electrical charges . We note that when  $z_s = z_0$  the electric charge is null .

The piezoelectric coefficient is  $d_{31}$  ( $CN^{-1}$ ),  $l_p$ ,  $a_p$  , are respectively length and thickness (m) of the piezoelectric bridge. We note that  $Q_F$  does not depend on the common width  $b_p = b_s = b_i$  of the structures (figure 4,5,6). This point is interesting and facilitates the technological realization of these structures since it limits the difficulties of their deep and straight engraving.



\*Another fundamental part of the functioning of this MEMS is the electronic description of switches (see figures 2, 3, and 4). These switches, indispensable for the functioning of the MEMS, are made with:

a/ We present Circuit n°1 (fig 2) made with T.F.T. MOS P and MOS N transistors enriched and in parallel: Threshold voltage  $V_{TNE}$  and  $V_{TPE}$



The common gates voltage of these enriched T.F.T. MOS N and P in parallel of switch n°1 (Red line figure 5), are controlled by the free mobile charges appearing on face n°2 of the piezoelectric bridge. 5).

Fig 2 : Circuit n°1: Switch n°1

The switch n°1 is made with two types of enriched MOSPE or MOSNE transistors in parallel, to avoid the exact nature (holes or electrons) of the mobile electric charges appearing on the metal face n°1 of the piezoelectric bridge. Preferably, their threshold voltages are the same in absolute value  $|V_{TNE}| = |V_{TPE}|$ .

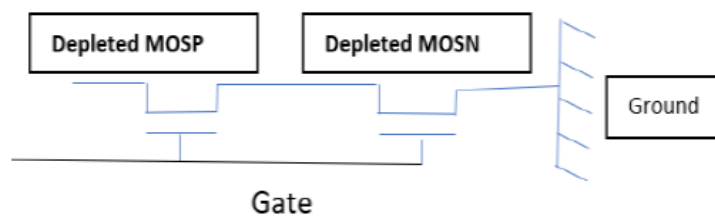


Fig 3 : Circuit 2: Switches n°2

The common gates of these MOS switches are controlled by the free charges appearing on face n°2 of the piezoelectric bridge. (Red line figure 2). The input of switch n°2 is connected to the Coulomb electrode, and its output to the RLC circuit, then to ground. Preferably, their threshold voltages are the same in absolute value  $|V_{TND}| = |V_{TPD}|$ .

The values of  $|V_{TND}| \approx |V_{TPD}|$  are lower but very close (down than 10%) of  $|V_{TNE}| \approx |V_{TPE}|$ .  
 Circuit n°2 (fig 3 and 4): with T.F.T. MOS P and MOS N transistors in depletion and in series: Threshold voltage  $V_{TND}$  and  $V_{TPD}$ .

An important point is that the threshold voltage values of these transistors are positioned as Figure 4.

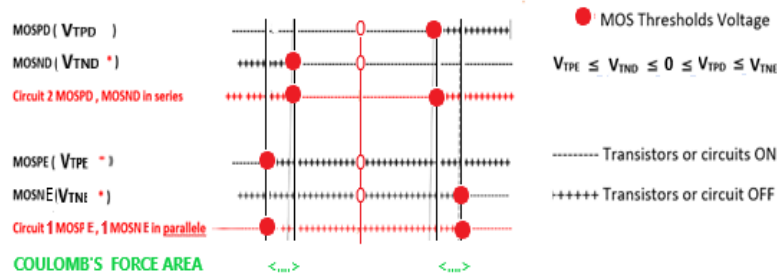


FIGURE 4 : Distribution of the threshold voltages of enriched and depleted n and p MOS switches. It is important to note that:

1/ The threshold voltage values of these switches are  $V_{T1}$  for switch n°1 ( fig 2 ) and  $V_{T2}$  for switch n°2 ( fig 3 ), and that  $|V_{T1}|$  is very slightly above  $|V_{T2}|$  with some tens of millivolts

2/ If the voltage on the insulating gates of the MOS TFT's is above their threshold voltage then: Switch n°1, changes from OPEN to CLOSED but conversely switch n°2 changes from CLOSED to OPEN ( Fig 4)

We have :  $V_{TPE} < V_{TND} < 0 < V_{TPD} < V_{TNE}$ . Consequently, as these threshold values have a difference of just some tens of millivolts then , switch n° 2 commute just before circuit switch n° 1.(see figure n° 2, 3, 4 ).

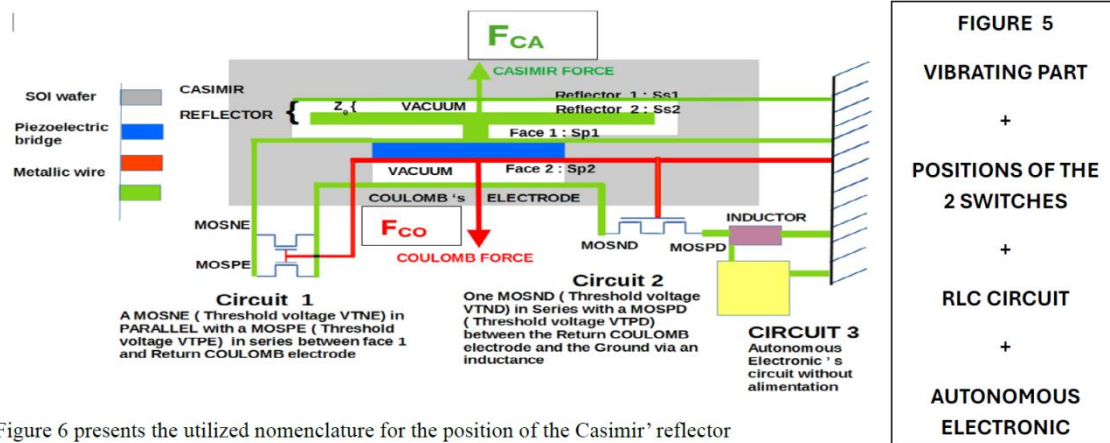


Figure 6 presents the utilized nomenclature for the position of the Casimir' reflector

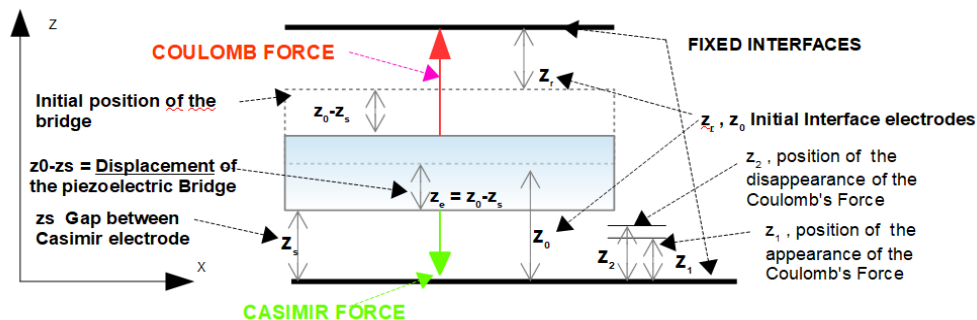


Figure 6: Axes, Forces, Casimir's Electrodes

At the starting point  $z_0$ , the electric charges of piezoelectric bridge are null, and the Coulomb electrode was grounded by the closing of switch n°2.(Fig 4, 5). Thus, Coulomb's force is null and only the perpetual, isotropic and timeless Casimir force  $F_{CA}$ , resulting from quantum vacuum fluctuations, causes the deformation of a microscopic piezoelectric. It deforms the piezoelectric bridge, and ionic charges appear in it .

As the deformation of the bridge is piezoelectric (Blue rectangle on figure 5 ) an electric field appears, ( due to the difference between the barycenter of the negatives and positives ions . This electrical field attracts from the mass, mobile charges of opposite signs on the two metalized faces of this bridge (green and red lines).

The mobile charge son face 2 of the piezoelectric bridge ( red line ) , generate on the insulating gates of the transistors Thin Film Transistor Metal Oxide Semiconductor T.F.T. M.O.S, a voltage  $V_G$  with the expression  $V_G = \frac{Q_F}{C_{ox}}$  . With,  $C_{ox}$  the capacity of the grid's transistors  $C_{ox} = \frac{\epsilon_0 \epsilon_{ox}}{t_{ox}} L_T W_T$ ,  $\epsilon_0$  the permittivity of vacuum,  $\epsilon_{ox}$  the relative permittivity of silicon oxide,  $L_T$ ,  $W_T$ ,  $t_{ox}$  respectively the length, width and thickness of the grid of the TFT MOS .

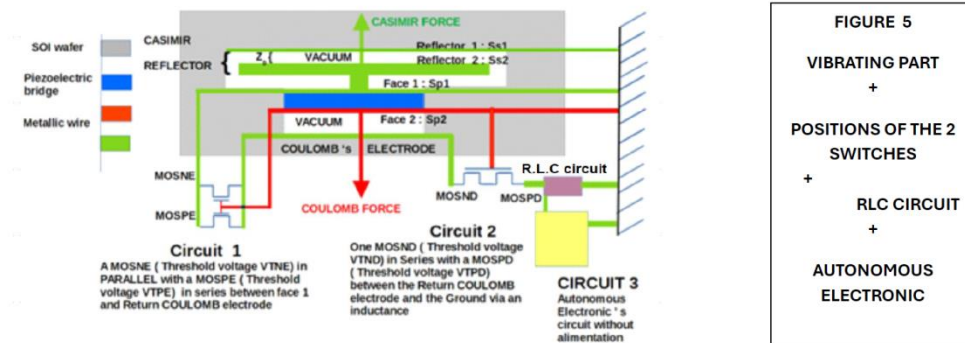
At the beginning:

1/ Switch number 1 is OPEN, isolating the electrode of face 1 (green) from the Coulomb's electrode. The mobile charges on face number 1 remain stationary and stay on this face (Fig. 5).

2/ Switch n°2 is CLOSED, grounding Coulomb's electrode.

When the gate voltage becomes equal to the threshold voltage, the switch n°1 CLOSE but switch n°2 keep OPEN .

Since there is no electric field on a perfect metallic electrode, the free-moving charges on face 1 must homogenize between the metallic film of face 1 and the metallic film of Coulomb's electrode (green line Fig. 5).Then, as the electrical nature of mobiles charges of faces n°1 and n°2 are opposite, a Coulomb's force  $F_{CO}$  must appear between these two metallic electrodes.



When the Coulomb return force  $F_{CO}$  is effective (switch n°1 CLOSED and switch 2 OPEN), it follows the law (fig 4,5,6)

$$F_{CO} = \frac{Q_F^2}{4 \pi \epsilon_0 \epsilon_r} \left( \frac{1}{z_r + z_0 - z_s} \right)^2 = \left[ \frac{d_{31} l_p}{a_p} S_s \frac{\pi^2 c \hbar}{240} \left( \frac{1}{z_s^4} - \frac{1}{z_0^4} \right) \right]^2 \left( \frac{1}{4 \pi \epsilon_0 \epsilon_r} \right) \left( \frac{1}{z_r + z_0 - z_s} \right)^2 \quad (\text{Eq. 3})$$

We note that  $F_{CO}$  is in  $1/z_s^{10}$ , with  $z_s$  = distance (time dependent) between Casimir electrodes, and  $z_0$  = initial distance between Casimir electrodes (without any electric's charges) .

The threshold voltages of the transistors of switch n°1, technologically predetermined, impose the intensity of Coulomb's forces, which can be much greater than the force of Casimir  $F_{CA}$ . So, the resulting force  $F_{CO} - F_{CA}$ , applied to the center of the piezoelectric bridge, changes direction or is zero. The elastic piezoelectric bridge necessarily returns (thanks to the stored deformation energy + the kinetic energy of the whole) to its initial position or a little above, therefore without any deformation or electrical charges.

The piezoelectric bridge straightens, its deformation decreases, the mobile charges on the electrodes drop, therefore the voltage  $V_g$  on the gates of switches 1 and 2 falls. Switch n°1 REOPENS very quickly; on the other hand, switch n°2 remains OPEN for a brief moment due to its threshold voltage slightly lower ( some tens of millivolts). (Fig 4, 6)

The Coulomb force is short-lived due to the rapid decrease in gate voltage, which soon reaches the threshold voltage of switch n°2. Consequently, this switch CLOSES to ground, thereby neutralizing the Coulomb force.

So, the positions  $z_1$  and  $z_2$  where the Coulomb force appears and disappears are very close. Consequently, the energy  $W_{COULOMB}$  expended by the Coulomb force between  $z_1$  and  $z_2$  remains low compared to that expended by the Casimir force for its translation from  $z_0$  to  $z_1$ . Consequently, the energy expended by the Coulomb force between  $z_1$  and  $z_2$  remains low compared to that expended by the Casimir force for its translation from  $z_0$  to  $z_1$ :

$$W_{COULOMB} = W_{FC0} = \int_{z_2}^{z_1} F_{C0} dz = \left\{ S_S \cdot \frac{\pi^2 \hbar c}{240} \cdot \frac{d_{31} l_p}{a_p} \right\}^2 \left( \frac{1}{8 \pi \epsilon_0 \epsilon_r} \right) \cdot \int_{z_2}^{z_1} \left[ \left( \frac{1}{z_s^4} - \frac{1}{z_0^4} \right) \left( \frac{1}{z_r + z_0 - z_s} \right) \right]^2 dz \quad \text{Eq 4}$$

$$W_{CASIMIR1} = \int_{z_0}^{z_1} F_{CA} dz = \int_{z_0}^{z_1} S \frac{\pi^2 \hbar c}{240 z_s^4} dz_s = S \left( \frac{\pi^2 \hbar c}{720} \right) \left[ \frac{1}{z_1^3} - \frac{1}{z_0^3} \right] \quad \text{Eq 5}$$

We calculate with MATLAB the integral of the equation of  $W_{COULOMB}$  and  $W_{CASIMIR1}$  between  $z_1$  and  $z_2$  (Fig 7 )

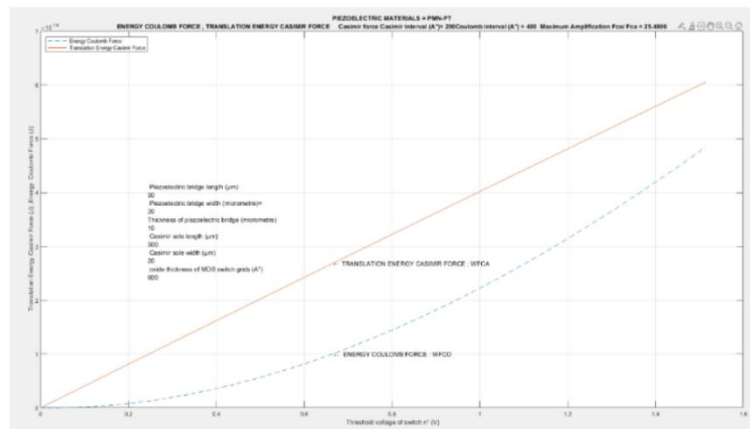


Fig 7:Energy of translation of Casimir Force and energy of Coulombs in function of the Threshold Voltage VT1 and VT2 of switches n°1 and n°2 VT2=VT1- 0.05 V Force between its apparition in the position  $z_1$  and its disappearance in position  $z_2$

To calculate  $z_s = z_1$  we simply write that  $z_1$  is the position where  $F_{CO} = p F_{CA}$  with  $p$  a chosen coefficient of amplification , that is :

$$F_{CO} = p F_{CA} \Rightarrow \frac{Q_F^2}{4 \pi \epsilon_0 \epsilon_r} \left( \frac{1}{z_r + z_0 - z_s} \right)^2 = \left[ \frac{d_{31} l_p}{a_p} S_S \frac{\pi^2 c \hbar}{240} \left( \frac{1}{z_s^4} - \frac{1}{z_0^4} \right) \right]^2 \left( \frac{1}{4 \pi \epsilon_0 \epsilon_r} \right) \left( \frac{1}{z_r + z_0 - z_s} \right)^2 =$$

$$p S_S \frac{\pi^2 c \hbar}{240 z_s^4} \quad \text{Eq 6}$$

We obtain the following curve which give the  $z_1$  apparition of the Coulomb's force  $F_{CO}$  in function of the force's amplification  $p = F_{CO}/F_{CA}$  (fig 8)

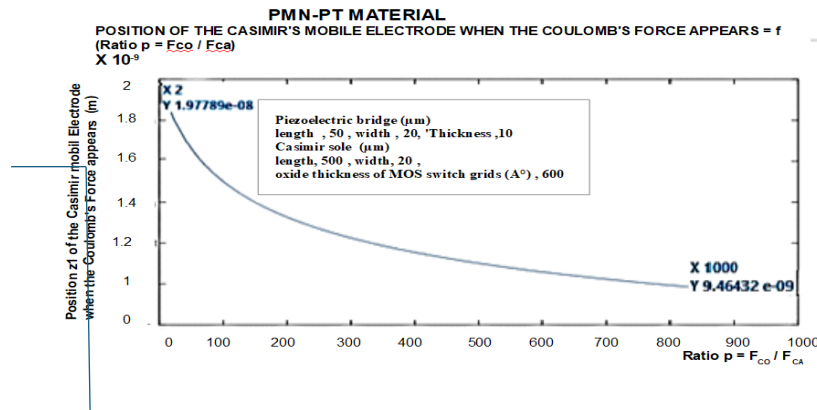


Fig. 8: Position of the mobile Casimir electrode  $z_1$  where the Coulomb force occurs:  $z_r = z_0 = 200 \text{ \AA}$ ,  $l_s = 500 \text{ \mu m}$ ,  $b_s = 20 \text{ \mu m}$ ,  $l_p = 50 \text{ \mu m}$ ,  $b_p = 20 \text{ \mu m}$ ,  $a_p = 10 \text{ \mu m}$

We can calculate easily the threshold voltage which induces the desired ratio amplification  $p = F_{CO}/F_{CA}$ . See figure 9

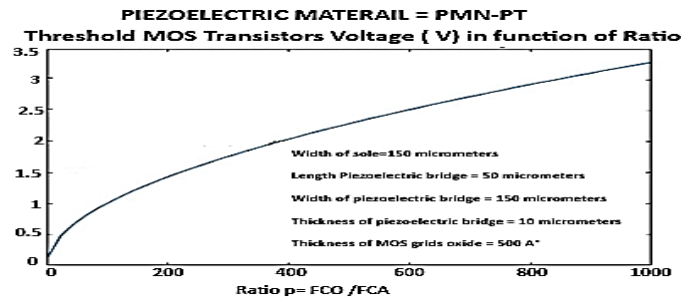


Figure 9: Materials = PMN-PT: Threshold voltage of the Enriched or Depleted MOS according to the  $F_{CO} / F_{CA}$  Ratio. Start interface =  $200 \text{ \AA}$

This ephemeral Coulomb force reduces, then cancels the deformation of the piezoelectric bridge, and thus its electric charges. The structure returns to its initial state and is again deformed by the timeless and isotope Casimir force  $F_{CA}$ , which always exists and is alone. (Fig 8). In Figure 10 we present the evolution of  $F_{CO}$  and  $F_{CA}$  when the interface  $z_s$  decreases from the initial position  $z_0$



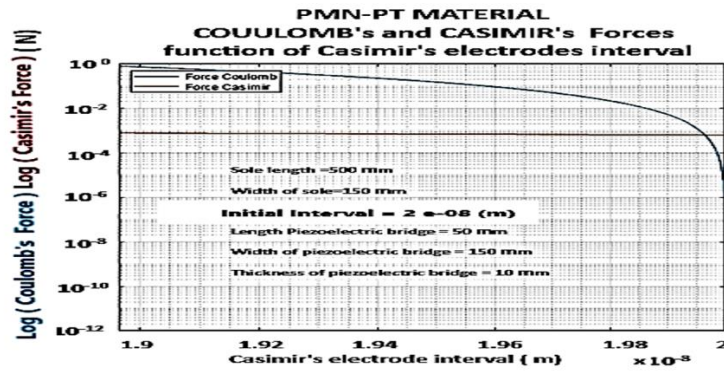


Figure 10: Materials =PMN-PT: Coulomb and Casimir force as a function of the inter-electrode interface.  
Start interface = 200A °

We remark that the  $F_{CO}$  intensity can quickly surpass the Casimir  $F_{CA}$  force, as shown on these  $F_{CA}$  and  $F_{CO}$  curves. The Coulomb's Force suppresses the collapse of the two very close electrodes of the Casimir reflector. When the Casimir sole deformed by the Casimir force  $F_{CA}$  reaches a position  $z_1$ , we note that switch n°2 is OPEN. (Fig 4,5)

This force  $F_{CO}$  is in the opposite direction to  $F_{CA}$  and can be much greater (Fig 10). The resultant  $F_{CO} - F_{CA}$  is in the opposite direction to the initial  $F_{CA}$  force and of greater intensity. The deformation of this bridge decreases, the electrical charges too. So, at position  $z_2$  of the mobile Casimir's reflector, the grid voltage appearing on the grids of switch n° 2 reaches its threshold voltage and it switches to CLOSED. Consequently, the Coulomb electrode is grounded via the R.L.C circuit (Fig 11), which implies that the mobile electrical charges and therefore the Coulomb force disappears.

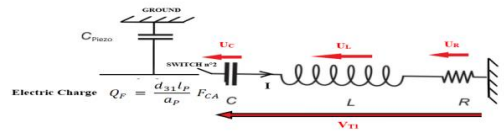


Fig 11 R.L.C. Circuit

However, even this very brief application of the Coulomb force gave the piezoelectric bridge and Casimir sole assembly kinetic energy and therefore inertia. This inertia of this assembly is slowed down by the still present Casimir force  $F_{CA}$  which now becomes a braking force for the assembly. The piezoelectric bridge then rises towards its initial position  $z_0$  and can even slightly exceed it depending on the value of the kinetic energy communicated by the force  $F_{CO}$ . (Fig 12)



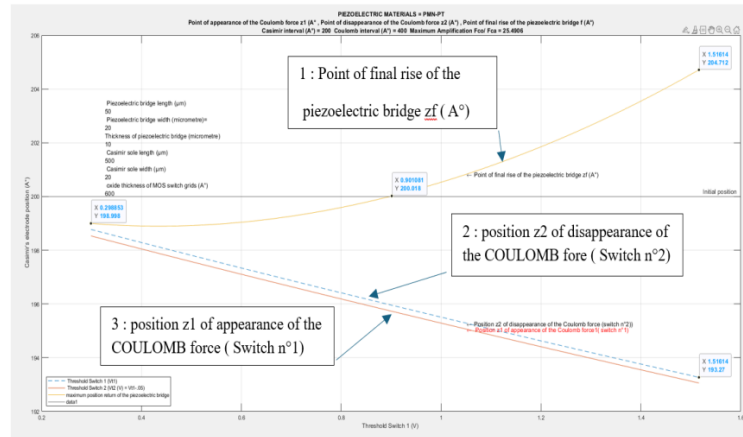


Fig 12: Positions of : 1/ The final rise  $z_f$  of the structure, 2/ of the point  $z_2$  of disappearance of the Coulomb force depending on the threshold voltage  $V_{T2}$  of switch  $n^{\circ}2$ , 3/ of the point  $z_1$  of appearance of the Coulomb force depending on the threshold voltage  $V_{T1}$  chosen for switch  $n^{\circ}1$

This cycle reproduces itself and the system vibrates (Fig 11,12,13) , with the vacuum energy transmitted by the  $F_{CA}$  force, as a continuous drive source for the deformation of the piezoelectric bridge and with the self-built Coulomb force  $F_{CO}$ , superior and opposed to  $F_{CA}$  as the counter-reaction force.

We obtain the following cyclic curves for different amplification  $p$  of the Coulomb's force  $F_{CO} = p F_{CA}$   
See fig 13 ,14 ,15

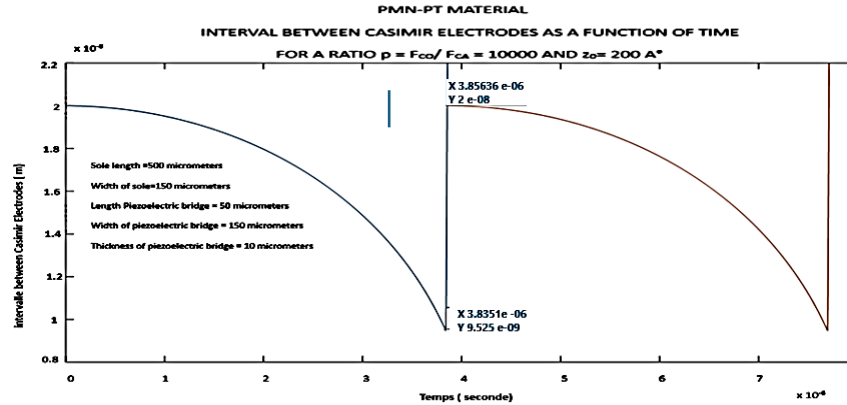


Figure 13: plot of the evolution of the Casimir inter-electrode interval as a function of time over two periods and an  $F_{co} / F_{ca}$  Ratio = 10000: Casimir inter-electrode interface = 200  $\text{\AA}$   
frequency vibration  $\approx 259336$  Hz

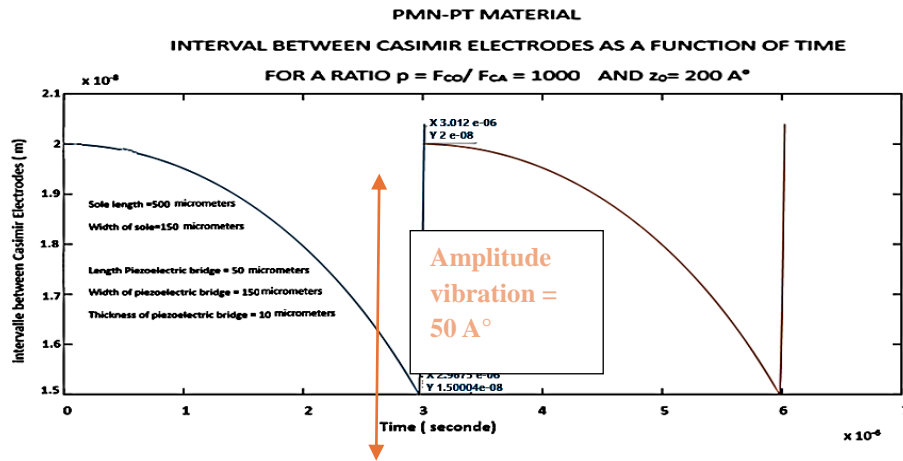


Figure 14: plot of the evolution of the Casimir inter-electrode interval as a function of time over two periods and Ratio  $F_{co} / F_{ca} = 1000$ : Casimir inter-electrode interface =  $200 \text{ A}^\circ$  frequency vibration  $\approx 333333 \text{ Hz}$

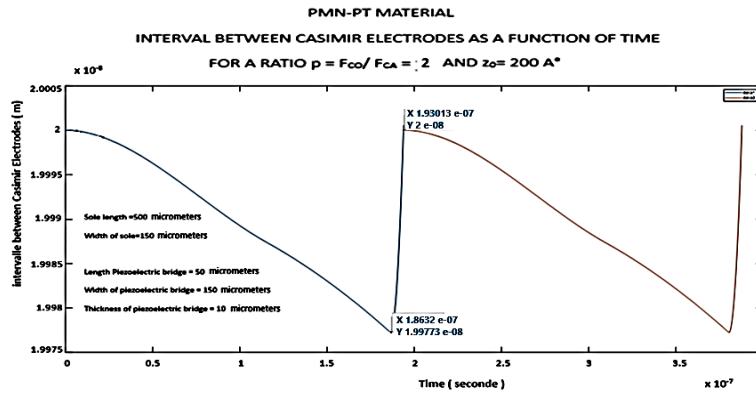


Figure 15: plot of the evolution of the Casimir inter-electrode interval as a function of time over two periods and a Ratio  $F_{co} / F_{ca} = 2$ . Casimir inter-electrode interface =  $200 \text{ A}^\circ$  frequency vibration  $\approx 55181347 \text{ Hz}$

At each cycle, the automatic switching of the integrated switches of circuits  $n^\circ 1$  and  $n^\circ 2$  distributes differently the mobile electrical charges located on face  $n^\circ 1$  of the bridge. Below we represent this cyclical vibration because it is permanently powered by vacuum energy (figure 16)

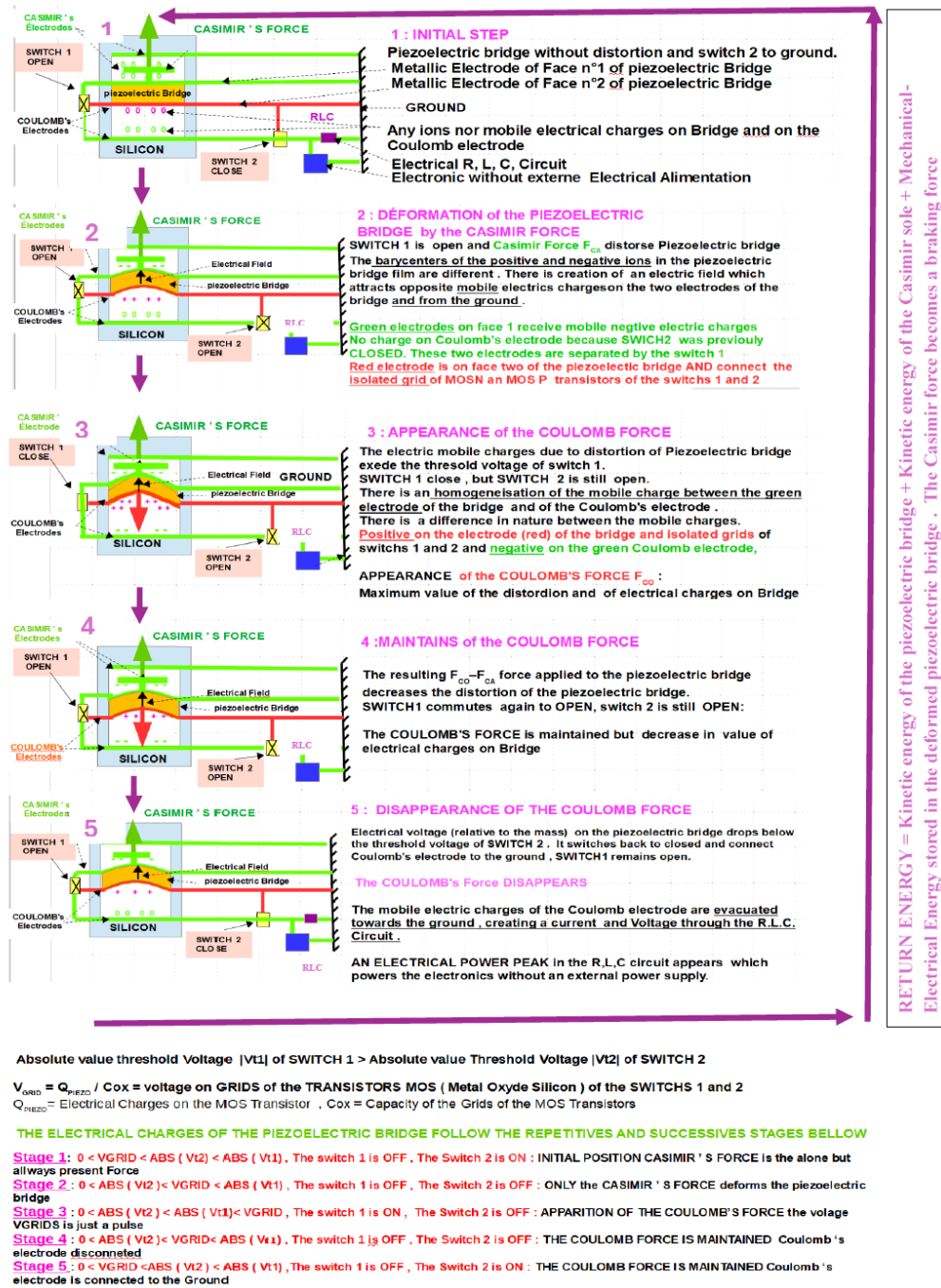


Fig 16 CYCLICAL VIBRATION OF THE MEMS

The moving part of the MEMS vibrates with amplitude and frequency influenced by the Casimir force and the Coulomb force, controlled by two switches, and its physico-geometric characteristics. For example, we can use PMN\_PT as piezoelectric material for the bridge, and the geometric characteristics of the MEMS of Fig 14 and moreover with the choice of a threshold voltage of 3.25 V for switch n°1 ( Fig 9 ) . Then these choices of physico-geometric characteristics induce an amplification ratio  $p = F_{CO} / F_{CA} = 1000$  ( fig 8 ) with a vibration amplitude of fifty Angstroms and a frequency of 333333 Hz.

We have also seen that at each vibration, the induced Coulomb force was of very short duration, thanks to the passage from OPEN to CLOSED of switch n°2. This switch n°2 connects the Coulomb electrode to ground via the RLC circuit in Figure 11. As a result, the electrical charges present on this Coulomb electrode are evacuated to ground. There is therefore for a brief instant a circulation of electrical charges in an RLC circuit which induces a current  $i(t)$ , a voltage  $U(t)$  and therefore an electrical power  $P(t)$ .

We will now calculate this electrical power and its energy at each vibration.

We will show in a future chapter the following and very important point: The balance of energies during the "OUT" and "RETURN" phases of the mobile structure satisfies the fundamental theorem of 1915 of the female mathematician EMMY NOTHER.

An RLC circuit is inserted between circuit n°2 and ground with an adjustment capacitance  $C$  in parallel with the capacity of the piezoelectric bridge  $C_{PIEZO}$  (Fig 17)

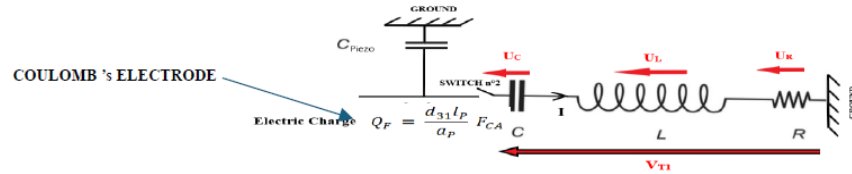


Figure 17 RLC circuit

With  $U_R = R I$ ,  $U_L = L d(I)/dt$ ,  $I = C d(U_C)/dt$  and  $R$  a resistance,  $L$  an inductance and  $C$  a capacity.

After rearranging we have the following equation  $\frac{d^2 U_C}{dt^2} + \frac{R}{L} \frac{dU_C}{dt} + \frac{U_C}{LC} = 0$ . **Eq 7**

With  $V_{T1} = \frac{Q_F}{C_{PIEZO}} = \frac{d_{31} l_p}{C_{PIEZO} a_p} F_{CA}$  = threshold voltage of switch n°1

This differential equation has solutions that depend on the value of its determinant  $\Delta$ .

We choose the values of  $R$ ,  $L$ ,  $C$  in such a way that the determinant  $\Delta = \sqrt{\left(\frac{R}{L}\right)^2 - \frac{4}{LC}} = 0$  of this equation is positive or vanishes.

So, if  $\Delta = 0$  the solution of the preceding differential equation is :

$$x_1 = \frac{R}{2L} \left( -1 + \sqrt{1 - \frac{4L}{CR^2}} \right) = -\frac{R}{2L} \text{ and } x_2 = \frac{R}{2L} \left( -1 - \sqrt{1 - \frac{4L}{CR^2}} \right) = -\frac{R}{2L} \text{ then we have } x_1 = x_2 = -\frac{R}{2L} < 0$$

**The capacity voltage**  $= u_c = \frac{V_{T1}}{x_1 - x_2} [x_1 \exp(x_2 t) - x_2 \exp(x_1 t)]$ , **Eq8**

**The capacity current**  $i_c = C \frac{du_c}{dt} = C \frac{V_{T1} x_1 x_2}{x_1 - x_2} [\exp(x_2 t) - \exp(x_1 t)]$  **Eq 9**

**The Power**  $P(t) = u_c i_c = \left( \frac{V_{T1}}{x_1 - x_2} \right)^2 C x_1 x_2 [\exp(x_2 t) - \exp(x_1 t)] [x_1 \exp(x_2 t) - x_2 \exp(x_1 t)]$  **Eq 10**

We obtain the following curves figure 18,19,20

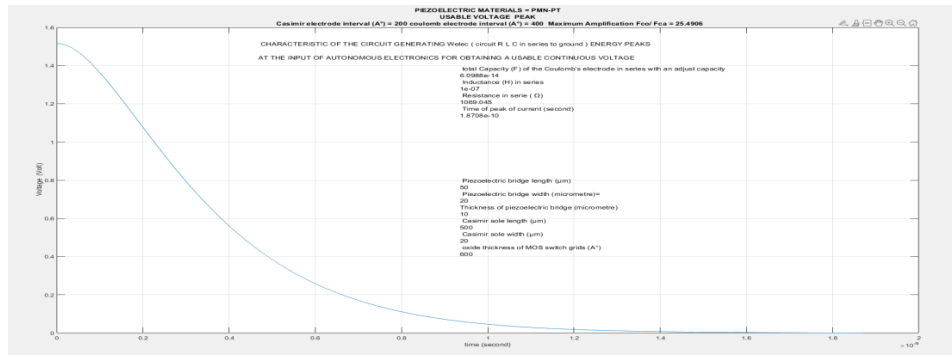


Fig 18 : Electric voltage on the capacitance C in series with the capacitance of the Coulomb electrode

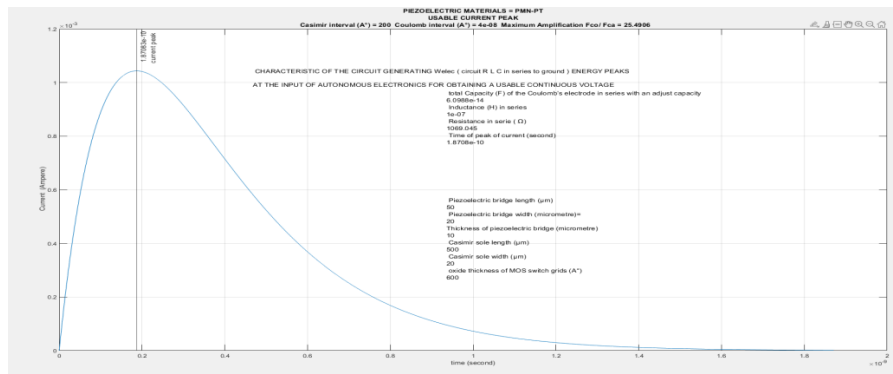


Fig 19 : The electric current flowing through the capacitance C in series with the capacitance of the Coulomb electrode

The peak of current is given when  $d(i_c)/dt = 0$  so at the time  $t_{imax} = \frac{\ln\left(\frac{x_2}{x_1}\right)}{x_1 - x_2} = \frac{\ln\left(\frac{1 + \sqrt{1 - \frac{4L}{CR^2}}}{1 - \sqrt{1 - \frac{4L}{CR^2}}}\right)}{\frac{R}{L} \sqrt{1 - \frac{4L}{CR^2}}} \text{Eq}$

11

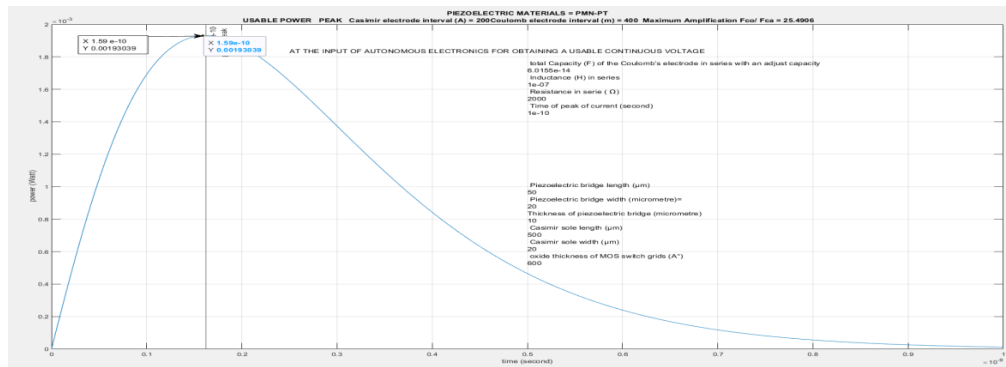


Fig 20: electrical power of the signal to power the autonomous electronics

The power  $P(t)$  is :  $P(t) = u_c i_c = \left(\frac{V_{T1}}{x_1 - x_2}\right)^2 C x_1 x_2 [\exp(x_2 t) - \exp(x_1 t)][x_1 \exp(x_2 t) - x_2 \exp(x_1 t)] \text{Eq 10}$

A part of this power is sent to the autonomous electronic ( fig 21).The peak power of 1.93 mW ( fig 20) is sufficient to power the autonomous electronics we present now and obtain a useful

voltage of several volts in a few milliseconds.( fig 22) The period of a vibration with for example the amplification ration  $p = F_{CO} / F_{CA} = 2$  , being (fig 15) of  $0.2 \mu s$ , the average power over a period is then approximately  $\approx 0.3 \mu W$ .

## 2. IN THIS PART WE PRESENT AUTONOMOUS ELECTRONICS TO TRANSFORM THE CYCLIC POWER PEAKS FROM THE R.L.C CIRCUIT

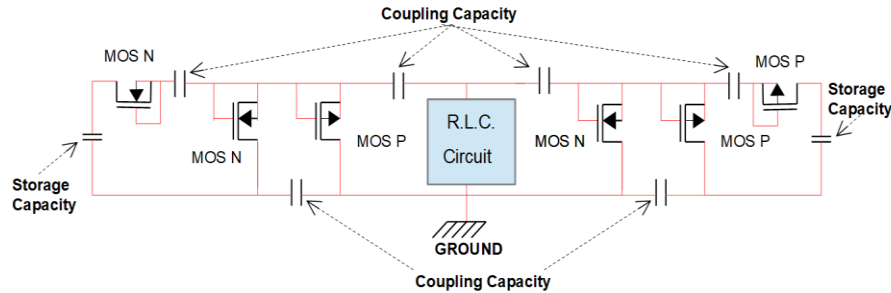


Figure 21: Principle of the single-stage doubler without power supply electrical diagram. All the MOS are isolated from each other by etching on an S.O.I wafer, and their threshold voltage is as close as possible to ground

The circuit of the figure 21 is an autonomous device operating without any electrical power source. It rectifies and accumulates the repetitive peak power delivered by the terminals of the RLC circuit in figure17 and transforms them into a usable direct voltage source. We notice in the following figure 22 that this autonomous electronics consumes - to operate - only a low power (at the start 60 nW and at the end 3 pW) coming from the RLC circuit. This RLC circuit is perfectly capable of providing it since it has a peak power of order of 2 mW (figure 20). We also note that the output of this autonomous electronics is a continuous voltage of several volts coming from a power peak at a frequency of 200 kHz

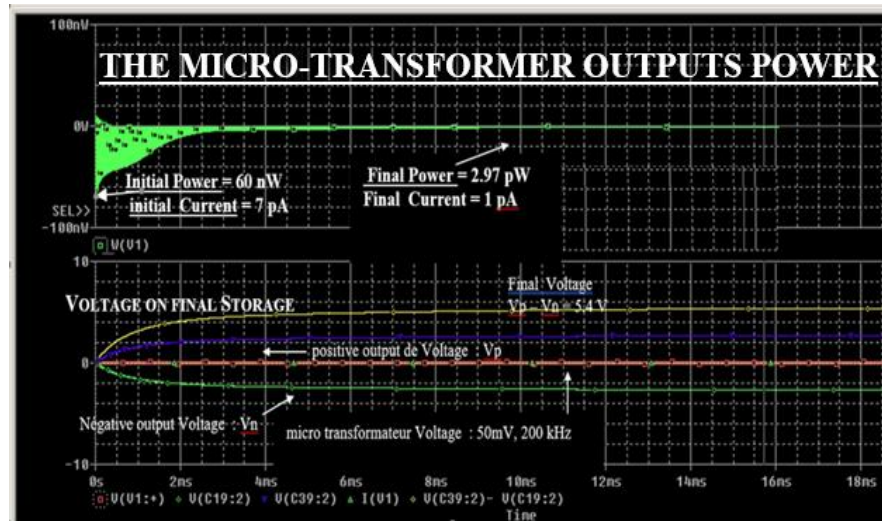


Figure 22: SPICE simulations of voltages, current, power consumed by the autonomous electronics for the transformation into direct voltage (5.4 V) of an alternating input signal of 50 mV, frequency = 150 kHz, number of stages = 14, coupling capacities = 20 pF, storage capacity = 10 nF.

We note the extreme weakness of the electrical power required at the start of the conversion of the power peaks (60 nW) and at the end (2 pW). This transformation requires 4 ms .

The interesting points for the presented autonomous electronics' device are:

- 1 / The low alternative input voltages required to obtain a continuous voltage of several volts at the output
- 2 / The low power and current consumed by this conversion and amplification circuit on the source which in this case is only an R.L.C. circuit, supplied by the current peaks generated by the autonomous vibrations.
- 3 / The rapid time to reach the DC voltage (a few tens of milliseconds)

Simply, the output impedance of this autonomous circuit must be large and can be made up with the input of a self-powered follower

We propose to use the technology CMOS, on intrinsic S.O.I. and with each element TFT MOSNE and TFT MOSPE transistors isolated from each other on independent islands to strongly limits the leakage currents. All these TFT MOS transistors have the lowest possible threshold voltages . See the following figure 23.

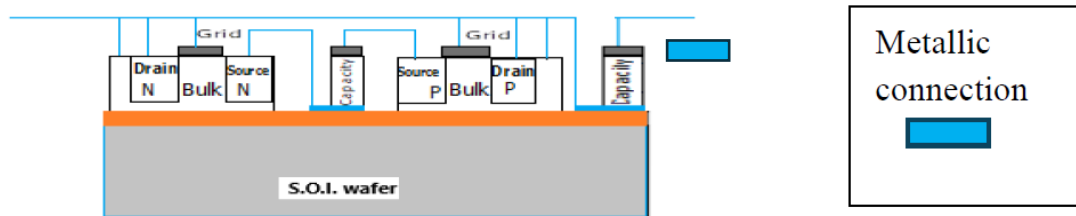


Figure 23: S.O.I technology for making the elements of the “doubler”

We note that, the choose coupling capacities of 20 pF of this electronic, like that of storage of the order of 10 nF, have relatively high values. To minimize the size of these capacitor we propose to use titanium metal for connectors and titanium dioxide as insulator. This oxidized metal with a relative permittivity of the order of 100 is one of the most important for a metal oxide. Then for a capacity of 20 pF the size of a square capacity passes to 15 $\mu$ m for a thickness of TiO<sub>2</sub> = 500 Å, which is more reasonable.

### 3. EQUATION DESCRIBING THE MECHANICAL AND ELECTRICAL BEHAVIOR OF THE MEMS PROPOSED TO EXTRACT ELECTRICAL ENERGY FROM THE QUANTUM VACUUM

In the following part we present some relatively simple equations which have allowed the preceding conclusions

- 1/ Let us calculate the evolution in time of the deflection of the piezoelectric bridge due to the forces which is applied in the middle of the bridge ( fig 24).



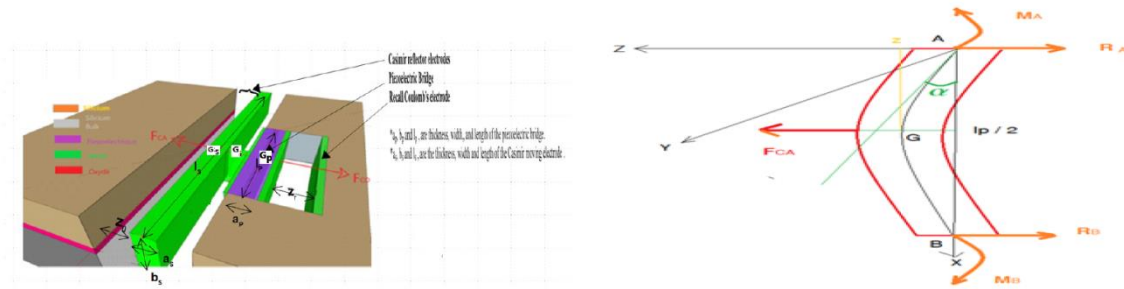


Figure 24: Piezoelectric bridge Cutting Reactions and Bending Moment, Deflection

We use the theorem of angular momentum for this vibrating structure.(Eq. 12)

$$\overrightarrow{\sigma_{Ax,y,z}^S (\text{Structure})} = \overrightarrow{I_{Ax,y,z}^S} \overrightarrow{\theta_{Ax,y,z}^S} \quad (\text{Eq. 12})$$

With  $\overrightarrow{\sigma_{Ax,y,z}^S}$  the angular momentum vector of the structure,  $\overrightarrow{I_{Ax,y,z}^S}$  the inertia matrix of the total structure with respect to the reference (A, x,y,z) and  $\overrightarrow{\theta_{Ax,y,z}^S}$  the rotation vector of the piezoelectric bridge with respect to the axis Ay with  $\alpha$  the low angle of rotation along the y axis of the piezoelectric bridge

$$\overrightarrow{\theta_{Ax,y,z}^S} = \begin{pmatrix} 0 \\ d\alpha/dt \\ 0 \end{pmatrix} \text{ with } d\alpha/dt \approx \frac{2}{l_p} \frac{dz}{dt} \text{ because } \sin(\alpha) = \sin\left(\frac{2z_s}{l_p}\right) \approx \frac{2z_s}{l_p}$$

We have (fig 24 ):

$l_p$  Eq (13)

Let  $G_p, G_i, G_s$  are the barycentre points respectively of the piezoelectric bridge, the connecting metal finger and of the metal block constituting the mobile sole of the Casimir reflector.

We have:

$$\begin{aligned} \overrightarrow{AG_{P,x,y,z}} &= \frac{1}{2} \begin{pmatrix} l_p \\ b_p \\ a_p \end{pmatrix} \xrightarrow{AG_{I,x,y,z}} = \frac{1}{2} \begin{pmatrix} l_p + l_i \\ b_p + b_i \\ a_p + a_i \end{pmatrix} \\ \overrightarrow{AG_{S,x,y,z}} &= \frac{1}{2} \begin{pmatrix} l_p + l_i + l_s \\ b_p + b_i + b_s \\ a_p + a_i + a_s \end{pmatrix} \end{aligned}$$

The inertia matrix of the bridge, in the frame of reference (Gp, x, y, z) is:

$$I_{GP}^P = \frac{m_p}{12} \begin{pmatrix} a_p^2 + b_p^2 & 0 & 0 \\ 0 & l_p^2 + b_p^2 & 0 \\ 0 & 0 & a_p^2 + l_p^2 \end{pmatrix} \quad \text{Eq14}$$

Taking Huygens' theorem into account, this inertia matrix becomes

$$I_{A,x,y,z}^P = m_P \begin{pmatrix} \frac{a_p^2 + b_p^2}{3} & -\frac{l_p b_p}{4} & -\frac{l_p a_p}{4} \\ -\frac{l_p b_p}{4} & \frac{a_p^2 + l_p^2}{3} & -\frac{a_p b_p}{4} \\ -\frac{l_p a_p}{4} & -\frac{a_p b_p}{4} & \frac{l_p^2 + b_p^2}{3} \end{pmatrix}$$

With the same reasoning we can calculate the inertia matrix of the finger  $I_{A,x,y,z}^I$  and the inertia matrix of the reflector  $I_{A,x,y,z}^C$  in the frame of reference (A, x, y, z),

$$I_{A,x,y,z}^I = \frac{m_i}{12} \begin{pmatrix} a_i^2 + b_i^2 & 0 & 0 \\ 0 & a_i^2 + l_i^2 & 0 \\ 0 & 0 & l_i^2 + b_i^2 \end{pmatrix} + m_i \begin{pmatrix} \frac{(b_p + b_i)^2 + (a_p + a_i)^2}{4} & -\frac{(b_p + b_i)(l_p + l_i)}{4} & -\frac{(a_p + a_i)(l_p + l_i)}{4} \\ -\frac{(b_p + b_i)(l_p + l_i)}{4} & \frac{(l_p + l_i)^2 + (a_p + a_i)^2}{4} & -\frac{(b_p + b_i)(a_p + a_i)}{4} \\ -\frac{(a_p + a_i)(l_p + l_i)}{4} & -\frac{(b_p + b_i)(a_p + a_i)}{4} & \frac{(b_p + b_i)^2 + (l_p + l_i)^2}{4} \end{pmatrix}$$

$$I_{A,x,y,z}^C = \frac{m_s}{12} \begin{pmatrix} a_s^2 + b_s^2 & 0 & 0 \\ 0 & a_s^2 + l_s^2 & 0 \\ 0 & 0 & l_s^2 + b_s^2 \end{pmatrix} + m_s \begin{pmatrix} \frac{(b_p + b_i + b_s)^2 + (a_p + a_i + a_s)^2}{4} & -\frac{(l_p + l_i + l_s)(b_p + b_i + b_s)}{4} & -\frac{(l_p + l_i + l_s)(a_p + a_i + a_s)}{4} \\ -\frac{(l_p + l_i + l_s)(b_p + b_i + b_s)}{4} & \frac{(l_p + l_i + l_s)^2 + (a_p + a_i + a_s)^2}{4} & -\frac{(b_p + b_i + b_s)(a_p + a_i + a_s)}{4} \\ -\frac{(l_p + l_i + l_s)(a_p + a_i + a_s)}{4} & -\frac{(b_p + b_i + b_s)(a_p + a_i + a_s)}{4} & \frac{(b_p + b_i + b_s)^2 + (l_p + l_i + l_s)^2}{4} \end{pmatrix}$$

The total inertia of the structure becomes in the reference (A, x, y, z) is :  $I_{A,x,y,z}^S = I_{A,x,y,z}^P + I_{A,x,y,z}^I + I_{A,x,y,z}^C$  with A at the edge of the recessed piezoelectric bridge .The angular momentum theorem applied to the whole structure gives :

$$\frac{d(\sigma_{A,x,y,z}^S)}{dt} = I_{A,x,y,z}^S \frac{d\theta_A^S}{dt} \Rightarrow I_{A,x,y,z}^S \frac{2}{l_P} \begin{pmatrix} 0 \\ \frac{d^2 z}{dt^2} \\ 0 \end{pmatrix} = \sum_A \overrightarrow{\text{Moments of the structure}} =$$

$$= \overrightarrow{M_A} + \overrightarrow{M_B} + \overrightarrow{F_{CA}} \wedge \begin{pmatrix} l_P/2 \\ 0 \\ 0 \end{pmatrix} \text{ with } \overrightarrow{F_{CA}} = \begin{pmatrix} 0 \\ 0 \\ F_{CA} \end{pmatrix}$$

**Eq 15**

The structure rotates around the Ay axis

We know [10]that the moments of a bridge with a force  $F_{CA}$  applied in its middle is at point A :  $M_{AY} = M_{BY} = -F_{CA} l_P / 8$ , therefore the summation of Moments on the structure relative to the axe Ay =  $1/4 * l_P * F_{CA}$ .

So, any calculation done; we obtain:  $I_y^S \frac{2}{l_P} \frac{d^2 z}{dt^2} = \frac{l_P}{4} F_{CA} = \frac{l_P}{4} S_S \frac{\pi^2 \hbar c}{240 z^4}$

With  $I_y^S$  the inertia of the structure relatively to the axe Ay.

$$I_Y^S = \rho_P a_P b_P l_P \left( \frac{(l_P^2 + a_P^2)}{12} + \frac{(l_P^2 + a_P^2)}{4} \right) + \rho_i a_i b_i l_i \left( \frac{(l_i^2 + a_i^2)}{12} + \frac{(l_P + l_i)^2 + (a_P + a_i)^2}{4} \right) + \rho_s a_s b_s l_s \left( \frac{(l_s^2 + a_s^2)}{12} + \frac{(l_P + l_i + l_s)^2 + (a_P + a_i + a_s)^2}{4} \right)$$

**Eq 16**

With  $\rho_P, \rho_i, \rho_s$ , respectively the densities of the piezoelectric bridge, the intermediate finger and the mobile electrode of the Casimir reflector.

By equation 17, we obtain the differential equation which makes it possible to calculate the interval between the two electrodes of the Casimir reflector as a function of time during the

"descent" phase when the Coulomb forces are not present  $\frac{d^2 z_S}{dt^2} = \frac{l_P^2}{8 l_Y^3} S_S \frac{\pi^2 \hbar c}{240 z_S^4}$  **Eq 17.**

This

differential equation unfortunately *does not have a useful literal solution, and we programmed it on MATLAB*. We calculate the duration of this "descent" of free Casimir electrode. This duration depends on the desired value of the proportionality coefficient  $p = F_{CO} / F_{CA}$ . (See figures 13,14,15).

Just at the closing switch n°1, we have  $F_{CO} = p F_{CA}$  with  $p$ , a coefficient of proportionality defined by the threshold voltages of the MOS interrupters.

At the end of "GOING" and before the start of the charge transfer, the total force  $F_T$  exerted becomes:  $F_T = F_{CA} - F_{CO} = F_{CA} (1-p)$ .

The "GOING" time of the free Casimir electrode will therefore stop when  $F_{CO} = -p F_{CA}$ .

We can calculate this point  $z_1$  where  $F_{CO} = p F_{CA}$ .

So, the "descent" of the free Casimir electrode stops when the inter electrode interface  $z_s = z_1$  is such that:

$$F_{CO} = p F_{CA} \Rightarrow \frac{Q_F Q_F}{8 \pi \epsilon_0 \epsilon_r} \left( \frac{1}{z_r + z_0 - z_1} \right)^2 = \left[ \frac{d_{31} l_P}{a_P} S_S \frac{\pi^2 \hbar c}{240} \left( \frac{1}{z_1^4} - \frac{1}{z_0^4} \right) \right]^2 \left( \frac{1}{4 \pi \epsilon_0 \epsilon_r} \right) \left( \frac{1}{z_r + z_0 - z_1} \right)^2 = p S \frac{\pi^2 \hbar c}{240 z_1^4} \quad \text{(Eq. (17)) See}$$

(Fig 25)

Fig 25 shows the point  $z_1$  where the Coulomb's force appears in function of the ratio  $p = F_{CO} / F_{CA}$

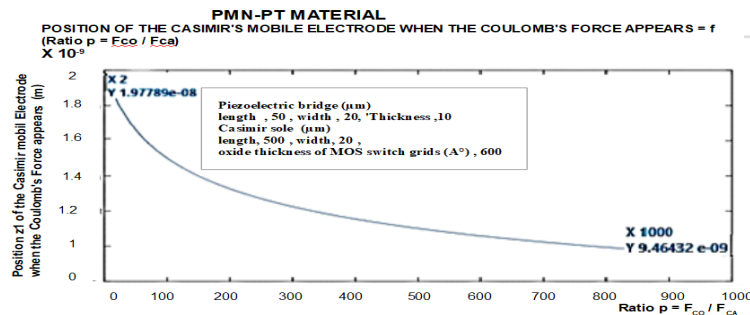


Fig. 25: Position of the mobile Casimir electrode  $z_1$  where the Coulomb force occurs :  $z_r = z_0 = 200 \text{ \AA}$ ,  $l_s = 500 \text{ \mu m}$ ,  $b_s = 20 \text{ \mu m}$ ,  $l_p = 50 \text{ \mu m}$ ,  $b_p = 20 \text{ \mu m}$ ,  $a_p = 10 \text{ \mu m}$

This programmable equation 17 gives the time  $t_d$  of the end of the "GOING" of the structure submitted to the Casimir force alone and :

a/ is calculable and will stop when the inter-electrode interface  $z_s$  has a value  $z_1$  satisfying equation (17)

b/ depend on the coefficient of proportionality  $p$ :

$$F_T = (1-p) F_{CA} \Rightarrow (1-p) S_s \frac{\pi^2 \hbar c}{240 z_{sm}^4} < 0 \text{ if } p > 1$$

When the Casimir reflector reaches position  $z_1$ , switch n°1 CLOSES and the COULOMB force appears.

During all the phase of the existing of the Force  $F_{CO}$ , so when  $0 < V_{TND} < V_{GRIDS} \leq V_{TNE}$ , or  $V_{TPE} \leq V_{GRIDS} < V_{TND} < 0$ . The total force, variable over time and exerted at the middle of the piezoelectric bridge, becomes:

$$F_T = F_{CA} - F_{CO} = S_s \frac{\pi^2 \hbar c}{240 z_s^4} - \frac{1}{2} \left[ \frac{S_s \pi^2 \hbar c}{240} \left( \frac{1}{z_s^4} - \frac{1}{z_0^4} \right) \left( \frac{d_{31} l_P}{a_P} \right)^2 \right] \left( \frac{1}{4 \pi \epsilon_0 \epsilon_r} \right) \left( \frac{1}{z_r + z_0 - z_s} \right)^2$$

**Eq. (18) .**

The piezoelectric bridge subjected to this new force  $F_T$  rises towards a position where the Coulomb's  $F_{CO}$ , disappears at the point  $z_2$  because the switch n° 2 closed to ground, via a R.L.C. circuit (fig 1,5) .

When  $F_{CO}$  disappears, the whole moving structure (Casimir reflector electrode + finger + piezoelectric bridge), so with a more important masse  $M_t$  than the bridge ,  $M_t = \rho_p(a_p b_p l_p) + \rho_i(a_i b_i l_i) + \rho_s(a_s b_s l_s)$  , acquires a kinetic energy  $E_c$  with  $E_c = \frac{1}{2} M_t V_t^2$ . With :  $V_t$ = speed of the mobile structures ,  $\rho_p$  ,  $\rho_i$ ,  $\rho_s$  ,  $a_p$   $b_p$   $l_p$  ,  $a_i$   $b_i$   $l_i$  ,  $a_s$   $b_s$   $l_s$  , respectively the volumic mass and the volume of the piezoelectric bridge, finger and Casimir electrode .

Let us calculate an approximation of the duration of this "rise"  $t_2$  of the mobile electrode Casimir's reflector + finger + piezoelectric bridge , triggered when  $F_{CO} = p F_{CA}$ .

This time  $t_2$  appears when the Coulomb force  $F_{CO}$  stop, with the closing of the switch n° 2 to ground, so at the point  $z_2$  between  $z_1$  and the initial point  $z_0$ , Fig 9.

Then, the mobile structure loses its kinetic energy  $E_c$  plus its deformation energy, thanks to the braking force provided by the Casimir force. This time is calculable rigorously, but, for this presentation, we approximate this return time by saying that point  $z_2$  of the loss of the Coulomb force occurs at the initial point  $z_0$ . The calculus of this time is easier and the error on this time duration is small. In these conditions, to know the time taken by the structure to "RETURN " to its neutral position, we must solve the following differential equation:

$$\frac{d^2 z}{dt^2} = \frac{l_P^2}{8 I_s^Y} (F_{CA} - F_{CO}) = \frac{l_P^2}{8 I_s^Y} \left\{ \left( l_s b_s \frac{\pi^2 \hbar c}{240 z_s^4} \right) - \frac{1}{2} \left[ l_s b_s \frac{\pi^2 \hbar c}{240} \left( \frac{d_{31} l_P}{a_P} \right) \left( \frac{1}{z_s^4} - \frac{1}{z_0^4} \right) \right]^2 \right\} \left( \frac{1}{4 \pi \epsilon_0 \epsilon_r} \right) \left( \frac{1}{z_r + z_0 - z_s} \right)^2$$

**Eq 19**

This differential equation (19) has no analytical solution and can only be solved numerically. We programmed it on MATLAB.

We present fig 26 the curve of these vibrations for a ratio  $p = 1000$

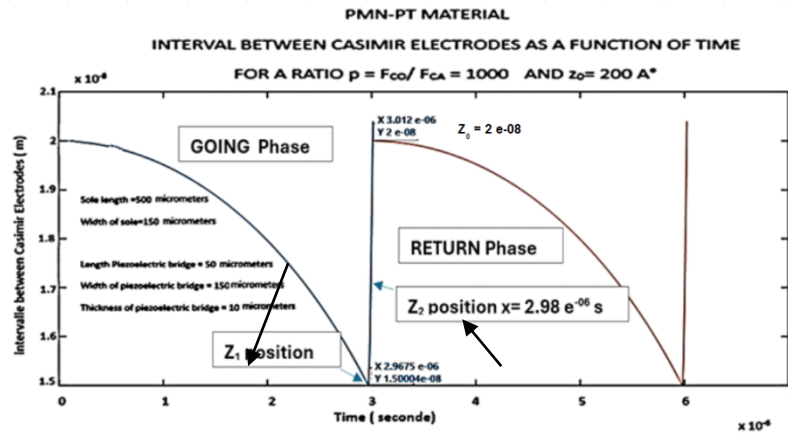


Figure 26: plot of the evolution of the Casimir inter-electrode interval as a function of time over two periods and with an implication  $p = F_{co} / F_{ca}$  Ratio = 1000: Casimir inter-electrode interface =  $200 \text{ A}^\circ$  frequency vibration  $\approx 333333 \text{ Hz}$

In these MATLAB simulations we considered that for technological important reasons, the metal of all electrodes and metal block was oxidized over a thickness allowing to have an interface between Casimir electrodes of  $200 \text{ A}^\circ$ . These considerations modifies the mass and the inertia of the vibrating structure (See technology part).

It turns out that the choice of aluminium as the metal deposited on these electrodes is preferable given:

- 1 / The ratio between the thickness of the metal oxide obtained and of the metal attacked by the thermal oxidation
- 2 / The low density of aluminium increase and optimise the vibration frequency of the structure by minimising the inertia of the Casimir reflector and the parallelepiped block that transfers the Casimir force.

The mass  $M_{\text{structure}}$  of the vibrating structure change and is know :

$$M_{\text{STRUCTURE}} = d_{\text{pm}} (a_s b_s l_s + a_i b_i l_i) + 2 d_{\text{om}} z_{\text{of}} (a_{s0} b_{s0} l_{s0} + a_{s0} l_{s0}) + d_p (a_p b_p l_p) .$$

With  $d_{\text{pm}}$  the density of the metal,  $a_s, b_s, l_s$  the geometries of the final metal part of the Casimir electrode sole,  $d_{\text{om}}$  the density of the metal oxide,  $a_{s0}, b_{s0}, l_{s0}$  the geometries of the oxidized parts around the 6 faces of the metal block,  $d_p$  the density of the piezoelectric parallelepiped (see figure 4,5):

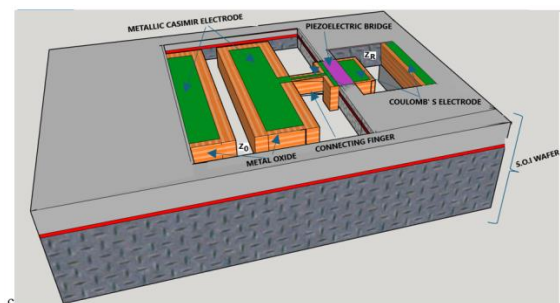


Figure 27: Drawing of the MEMS

#### 4. A MICRO TECHNOLOGY PROPOSAL TO REALIZE THIS MEMS TECHNOLOGY OF REALIZATION OF THE CURRENT EXTRACTOR DEVICE USING THE FORCES OF CASIMIR IN A VACUUM

##### Steps for the realization of the structure and its electronics

For the structures presented above, the space between the two surfaces of the reflectors must be

- be metallic to conduct the mobile charges
- insulating as stipulated by the expression of Casimir's law who is established for surfaces without charges.
- On the order of  $200 \text{ \AA}$ , ....which is not technologically feasible by engraving.

*Yet it seems possible to be able to obtain this parallel space of the order of  $200 \text{ \AA}$  between Casimir reflectors, not by etching layers but by making them thermally grow. This should be possible if we grow an insulator on the z direction of the structure, for example  $\text{Al}_2\text{O}_3$  or  $\text{TiO}_2$  or other oxide metal which is previously deposited and in considering the differences in molar mass between the oxides and the original materials.*

We use an SOI wafer with an intrinsic silicon layer : The realisation start with voltage "doubler" is obtained by using CMOS technology with 8 ion implantations on an SOI wafer to make :

- 1 / The sources, drains of the MOSNE, MOSND of the "doubler" and of the Coulomb force trigger circuits and of the grounding
  - 2 / The source, drains of the MOSPE, MOSPD of the "doubler" and of the Coulomb force trigger circuits
  - 3 / The best adjust the zero-threshold voltage of the MOSNE of the "doubler" circuit
  - 4 / The best adjust the zero-threshold voltage of the MOSPE of the "doubler" circuit
  - 5 / To define the threshold voltage of the MOSNE of the circuit n°1
  - 6 / To define the threshold voltage of the MOSPE of the circuit n°1
  - 7 / To define the threshold voltage of the MOSND of the circuit n°2
  - 8 / To define the MOSPD threshold voltage of the circuit n°2
- This electronic done, we take care of the vibrating structure of CASIMIR
- 9 / engrave the S.O.I. silicon to the oxide to define the location of the Casimir structures (figure 28)

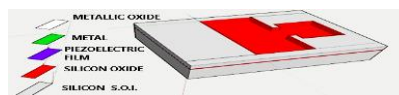


Figure 28 : 9/ etching of S.O.I silicon

- 10/ Place and engrave a protective metal film on the rearfaces of the S.O.I wafer (figure 230)



Figure 30: 10/ Engraving of the protective metal rear face of the S.O.I. silicon

11 / Deposit and engrave the piezoelectric layer (figure 31)

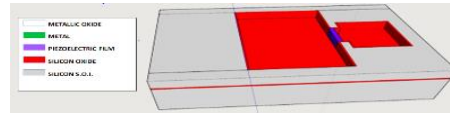


Figure31: 11/deposition and etching of the piezoelectric layer deposition and etching of the piezoelectric layer

12/ Depose and etch the metal layer of aluminium (figure 32) .

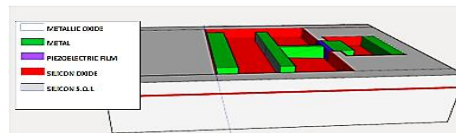


Figure 32: 12/ Metal deposit, Metal engraving etching of the piezoelectric layer

13 / Plasma etching on the rear side the silicon of the Bulk and the oxide of the S.O.I wafer protected by the metal film to free the Casimir structure then very finely clean both sides (figure 33)

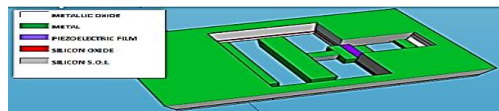


Figure 33: 13/ view of the Casimir device on the rear face, engraving on the rear face of the structures.

14 / Place the structure in a hermetic integrated circuit support box and carry out all the bonding necessary for the structure to function.

15 / Carry out the thermal growth of aluminium oxide  $Al_2O_3$  with a measurement and control of the circuit under a box. The electronic circuit should generate a signal when the interface between the Casimir electrodes becomes weak enough for the device to vibrate ... and then stop the oxidation.(Figure 34)



Figure 3: 15 /Adjusted growth of metal oxide under the electronic control, front view of the Casimir device

16 / Create a vacuum in the hermetic box

We remark that, in case where the 2 metal electrodes of Casimir reflector adhere to one another, we can try to separate them by the application of an electrical voltage on the Coulomb's electrodes.

We have presented very quickly 6 points :

1/ The principles used by this MEMS whose objective is to extract electrical energy from a completely unused source: the quantum vacuum.

2/ The mathematics associated with the operation of the vibrating part of this MEMS



- 3/ The computer calculations (MATLAB) of these equations
- 4/ The computer simulations (ANSYS) of this MEMS structure
- 5/ The electrical simulations (SPICE) of an autonomous and original electronics of amplification and storage in a continuous voltage of several Volts, of electrical signals from the MEMS
- 6/ We propose a micro, nanotechnology to fabricate the vibrating part and the autonomous electronic for this MEMS .

But , this presentation lacks the fundamental proof that this extraction of energy from the quantum vacuum is carried out according to the very important theorem of the mathematician EMMY NOETHER and that there is no creation of energy ex-nihilo but simply a transfer of the energy still unused but universal and timeless in our universe, that of the quantum vacuum. We will present now this very important part before concluding this presentation.

## 5. MEMS ENERGY BALANCE

In this part, we will try to make a detailed and exhaustive assessment of the behavior of the MEMS during one vibration.

Firstly, we will focus on the first half of this vibration, which we will call the "going" phase. Secondly, we will focus on the second half of the vibration, which is the "return" phase. Let us recall that, the piezoelectric bridge is perfectly elastic, which implies, as with any elastic structure, that the energy expended by a mechanical deformation from the positions from 0 to 1 is integrally restored when returning from 1 to 0 . We recall that the conditions of use of the piezoelectric bridge (vibrations amplitude) are in their purely elastic domain, and we never enter in the domain of plasticity.

In the following we propose to put into equation the energy balance of «go» then in “return” steps.

### 5.1. MEMS energy balance during the phase “GOING ” from $z_0$ to $z_1$

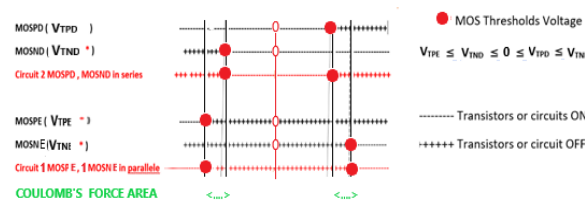
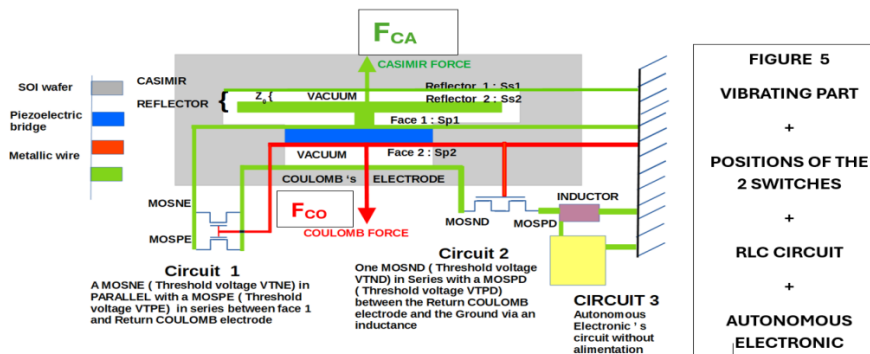


figure 4 : Distribution of the threshold voltages of enriched and depleted N and PMOS switches.  $V_{t1}$  : Threshold Voltage of SWITCH n°1 ,  $V_{t2}$  : Threshold Voltage of SWITCH n°2



**a/First part ( GOING part ) : Starting :  $0 < V_G < \text{abs}(V_{T2}) < \text{abs}(V_{T1})$  .: switch n°1 OFF, Switch n°2 ON.(Fig 1)**

At the start, we have very small deformations applied to the piezoelectric bridge. Consequently, the electrical voltages  $V_G$  on the grid of the enriched and parallel TFT MOS N and P of switch n°1 and n°2 is lower than their threshold voltage  $V_{T1}$ .and  $V_{T2}$

Theswitch n°1 is OPEN. On the other hand, as  $V_G < V_{T2}$ , switch n°2 consisting of two TFT MOS N and P in series, operating in depletion mode is CLOSED and connect the Coulomb's electrode to ground, thus eliminating the Coulomb force  $F_{CO}$

**b/ ( GOING part ) :  $0 < \text{abs}(V_{T2}) < V_G < \text{abs}(V_{T1})$ . and  $F_{CO} / F_{CA} < p$ : Switch n°1 OFF, Switch n°2 ON or OFF. (Fig 1)**

The electric moving charges of the face n°1 are isolated by the OPEN switch n°1. Any electric charge on the return side of the Coulomb electrode. The Casimir force begins to deform the piezoelectric bridge more significantly.

1/ Note that the mobile parallelepiped metal electrodes of the Casimir electrodes remain parallel to each other and that the mobile metal Casimir electrode does not deform.

2/ The expulsion of entropy  $\Delta S$  from the vibrating structure of Casimir (movements of its internal atoms) is transmitted to the piezoelectric bridge by heat . In first approximation, we can use the well-known formula  $\Delta Q_{vib} = \Delta S \cdot \Delta T$ , with  $\Delta S$ = entropy variation ( $J \cdot ^\circ K^{-1}$ ) , $\Delta Q_{vib}$  the heat transmitted by the vibrations and  $\Delta T$ = temperature variation ( $^\circ K$ )

However, we know that:  $\Delta Q_{vib} = \frac{M_{Bridge} [2 \pi f_{vib}]^2}{2} z_1^2 = M_{Bridge} \cdot C_{piezo} \Delta T$  **Eq. (20)**

With:  $f_{vib}$ = Vibration frequencies of the piezoelectric bridge,  $M_{Bridge}$  = mass of this bridge, which is the only one to deform because the Casimir electrodes are simply in translations. We note  $z_1$  the maximum deflection of the bridge,  $C_{piezo}$  = Specific heat capacity of the piezoelectric bridge ( $J \cdot Kg^{-1} \cdot ^\circ K^{-1}$ ),  $\Delta T$  = Temperature variation ( $^\circ K$ ).

Consequently  $\Delta T = \frac{2 [\pi f_{vib}]^2}{C_{piezo}} z_1^2$  **Eq. (21)**= Temperature variation of the bridge. . For example,

for a PMN-PT piezoelectric film:  $C_{piezo} = C_{PMN-PT} = 310 (J \cdot Kg^{-1} \cdot ^\circ K^{-1})$ ,  $f_{vib} \approx 10^6 \text{ Hz}$ ,  $z_1 \approx 100 \cdot 10^{-10} \text{ m}$ ,  $\Delta T \approx 10^{-3} \cdot ^\circ K$ .

**The expulsion of entropy from the vibrating Casimir Electrode is negligible.**

Half of this expended heat occurs in the “GOING” phase, the second part occurs in the “RETURN ” phases of the vibration.

It is very important to remark that, to deform the elastic piezoelectric bridge from  $z_0$  to  $z_1$  , during the displacement " GOING" of the vibration , **the quantum energy  $E_{CASIMIR1}$**  , given by the quantum vacuum , is used for **four different energies**:

1/ The energy used for the simple displacement from  $z_0$  to  $z_1$  of the point of application of the Casimir force:  $W_{CASIMIR1}$

2/ The mechanical energy for the deformation of the elastic bridge:  $W_{DEFCA1}$

3/ The energy to create the fixed ionic charges  $Q_F$  in this piezoelectric structure :  $W_{BRIDGE}$

4/ The expulsion of entropy  $\Delta S/2$  energy, expended in heat due to the friction of the atoms in the half of the vibration of the bridge heat :  $\Delta Q_{vib}/2$

The quantum vacuum energy  $E_{CASIMIR1}$  must provide all these preceding energies and is greater than the simple translation energy  $W_{CASIMIR1}$ . The energies  $W_{DEFCA1}$  and  $W_{BRIDGE1}$  are **store in the** deformed piezoelectric bridge as a potential energy.

We can write that to deform the piezoelectric bridge from the start position  $z_0$  to the position  $z_1$  the vacuum provides the energy

$$E_{GOING} = E_{CASIMIR1} = W_{CASIMIR1} + W_{DEFCA1} + W_{BRIDGE1} + \Delta Q_{vib}/2, \text{ (Eq 22).}$$

1/ The **translation energy**  $W_{CASIMIR1}$  of the Casimir force  $F_{CA}$  from  $z_0$  to  $z_1$  is :

$$W_{CASIMIR1} = \int_{z_0}^{z_1} F_{CA} dz = \int_{z_0}^{z_1} S \frac{\pi^2 \hbar c}{240 z_s^4} dz_s = S \left( \frac{\pi^2 \hbar c}{720} \right) \left[ \frac{1}{z_1^3} - \frac{1}{z_0^3} \right] \text{ (Eq 23).}$$

Now, let's calculate the deformation energy  $W_{DEFCA1}$  of the piezoelectric bridge fixed at both ends. All Material Resistance book says that the deformation energy  $W_d$  of an embedded elastic bridge and for a constant force F is :  $W_d = \frac{1}{2} (z_0 - z_s) \cdot F$ .

In the case of our piezoelectric bridge the force F being the Casimir force, varies in  $1/z_s^4$ , with the distance  $z_s$ . So, for a differential deflection  $dz$  of the bridge under the force  $F(z)$  we can write :

$$d(W_d) = \frac{1}{2} F(z) dz \Rightarrow W_d = \frac{1}{2} \int_{z_0}^{z_1} F(z) dz = W_{DFCA1}(z_s) = \frac{1}{2} S \frac{\pi^2 \hbar c}{240} \int_{z_0}^{z_1} \frac{1}{z^4} dz = \frac{1}{6} \frac{\pi^2 \hbar c}{240} \left[ \frac{1}{z_1^3} - \frac{1}{z_0^3} \right] \text{ (Eq 24).}$$

We notice that  $W_{DEFCA1} > 0$ . The numerical value of  $W_{DEFCA1}$  is a little smaller than the expression calculated if  $F_{CA}(z_1)$  was constant, Many RDM Book gives this expression  $W_d$  with :  $W_d = \frac{1}{2} z_e \cdot F_{CA}(z_1)$ . The reached position  $z_1$  is unstable because the Casimir force increases with its position. As a result, the mobile Casimir electrode can collapse.

When the Casimir electrode is in  $z_1$  position, the switch  $n^\circ 1$  switches to CLOSED. Note that, when switch  $n^\circ 1$  commutes, switch  $n^\circ 2$  is still OPEN) fig 4.

The charges present on the metallic face  $n^\circ 1$  of the piezoelectric bridge must homogenize with the metallic Coulomb electrode which is to ground just before because there is no electrical field in a perfect conductor. These mobile electrical charges create an ephemeral Coulomb's  $F_{CO}$  force, but bigger than  $F_{CA}$ .

2/ During the displacement " GOING " the total energy  $E_{CASIMIR}$  is also used to generate a potential energy  $W_{BRIDGE}$  accumulated in the capacity of this piezoelectric bridge which follows the equation:

$d(W_{BRIDGE}) = Q_F d(V_{PIEZO})$  with  $V_{PIEZO}$  = Voltage between the two metallic faces of the piezoelectric bridge, and  $d(Q_F) = C_{PIEZO} d(V_{PIEZO})$ . We obtain:

$$W_{BRIDGE1} = \int_0^{Q_1} \frac{Q_F}{C_{PIEZO}} d(Q_F) = \frac{1}{2 C_{PIEZO}} [Q_F^2]_0^{Q_1} = \frac{a_P}{2 l_P b_P \epsilon_0 \epsilon_{PIEZO}} \left[ \left( \frac{d_{31} l_P}{2 a_P} \right)^2 F_{CA}^2 \right]_{z_0}^{z_1} = \left( \frac{a_P}{2 l_P b_P \epsilon_0 \epsilon_{PIEZO}} \right) \left( \frac{d_{31} l_P l_s b_s \pi^2 c \hbar}{480 a_P} \right)^2 \left[ \frac{1}{z_1^4} - \frac{1}{z_0^4} \right] \text{ (Eq 26).}$$

We notice that this part  $W_{BRIDGE1}$  of  $E_{CASIMIR1} > 0$ , is stored in the piezoelectric bridge as potential energy.

$W_{DEFCA1}$  and  $W_{BRIDGE1}$  are potential energies that will be used when the elastic bridge returns to its equilibrium position, that is to say without deformation.

Let's call  $z_2$  the point between  $z_1$  and  $z_0$  where the Coulomb's force disappears.

There are two phases for the return to from  $z_1$  to  $z_0$  (RETURNING phase):

- 1/ Between  $z_1$  to  $z_2$  where the Coulomb's force  $F_{CO}$  exist and contribute to straighten the elastic structure and to give it kinetic energy,
- 2/ from  $z_2$  to  $z_0$  where this acquired kinetic energy, and the remaining energy still stored in the structure will be dissipated by the energy spent by the Casimir force.

## 5.2. MEMS energy balance during the “RETURN” phase from $z_1$ to $z_2$ , switch n°1 CLOSED, Switch n°2 OPEN: $0 < \text{abs}(V_{T2}) < V_G < \text{abs}(V_{T1})$ . And Ratio $F_{CO} / F_{CA} = p$ : (Fig 4)

The switch n°2 is still OPEN, so the Coulomb's electrode still exists. The values of  $V_{T2}$  and  $V_{T1}$  impose that  $z_2$  is very close to  $z_1$ .

So, the energy  $W_{COULOMB} = \int_{z_1}^{z_2} F_{CO} dz$  expended by the Coulomb force remains low, even if this force is several times that of Casimir in intensity. The time of existence of  $F_{CO}$  is of the order of a few tens of nanoseconds (fig 13,14,15).

### 5.2.1. Calculation of the COMLOMB's energies between $z_1$ and $z_2$ .

As soon as switch n°1 has switched to CLOSED, the resulting force  $F_{CO} - F_{CA}$  straightens this bridge and the electric charges drop. The electric voltage on the grids falls below the threshold voltage of this switch n°1 which commute again very quickly to OPEN. The energy  $W_{COULOMB}$  is write .

$$W_{COULOMB} = W_{FCO} = \int_{z_1}^{z_2} F_{CO} dz = \left\{ S_S \cdot \frac{\pi^2 \hbar c}{240} \cdot \frac{d_{31} l_p}{a_p} \right\}^2 \left( \frac{1}{8 \pi \epsilon_0 \epsilon_r} \right) \cdot \int_{z_1}^{z_2} \left[ \left( \frac{1}{z_s^4} - \frac{1}{z_0^4} \right) \left( \frac{1}{z_r + z_0 - z_s} \right) \right]^2 dz_s$$

**Eq27 .**

This Coulomb's energy exists only between the very close positions  $z_1$  and  $z_2$ . The literal formulation of  $W_{COULOMB}$  energy is possible but its expression is not convenient because it is too complex. We prefer to calculate by MATLAB its numerical value between the value  $z_1$  and  $z_2$ . The position  $z_2$  of commutation of switch n°2 is deduced from the chosen threshold value  $V_{T2}$  of switch n°2.

We note that we can minimize the value of the energy spent by  $W_{COULOMB}$ , by choosing a value of  $z_2$  near  $z_1$  so a threshold voltage  $V_{T2}$  of switch n°2, close but slightly lower than  $V_{T1}$  of switch n°1. For example  $V_{T2} = V_{T1} - 0.05$  (V).

We use MATLAB to find position  $z_2$  of commutation of circuit 2 to cancel Coulomb's Force  $F_{CO}$ . At position  $z_2$  of the bridge, the electric charge in the TFT MOS .

$$Q_2 = \frac{d_{31} l_p}{a_p} S_S \frac{\pi^2 \hbar c}{240} \left( \frac{1}{z_2^4} - \frac{1}{z_0^4} \right) \text{ with } Q_2 = C_{OX} V_{T2} \text{ . So , } z_2 = \frac{1}{\sqrt[4]{\left[ \frac{240 a_p C_{OX}}{d_{31} l_p \pi^2 \hbar c S_S} V_{T2} + \frac{1}{z_0^4} \right]}} \quad (\text{Eq .28}).$$

When the bridge reaches the position  $z_2$ , the memorized elastic energy is  $W_{DFCA2} = \frac{1}{6} S \frac{\pi^2 \hbar c}{240} \left[ \frac{1}{z_2^3} - \frac{1}{z_0^3} \right]$  (Eq 29).

. Similarly, the memorized elastic energy  $W_{BRIDGE2}$  occurs .

$$W_{BRIDGE2} = \int_0^{Q_2} \frac{Q_F}{C_{PIEZO}} d(Q_F) = \frac{1}{2 C_{PIEZO}} [Q_F^2]_0^{Q_2} = \frac{a_P}{2 l_P b_P \epsilon_0 \epsilon_{PIEZO}} \left[ \left( \frac{d_{31} l_P}{2 a_P} \right)^2 F_{CA}^2 \right]_{z_0}^{z_2} =$$

$$\left( \frac{a_P}{2 l_P b_P \epsilon_0 \epsilon_{PIEZO}} \right) \left( \frac{d_{31} l_P l_S b_S \pi^2 c}{480 a_P} \right)^2 \left[ \frac{1}{z_2^4} - \frac{1}{z_0^4} \right]^2 \quad (\text{Eq 30}).$$

We can calculate the energy spent in the first part of return of the structure (from  $z_1$  to  $z_2$ ) by simply calculating the kinetic energy  $W_{CIN}$  acquired by the structure when it reaches the position  $z_2$  upon its return. In fact, we know that the variation of the kinetic energy  $W_{CIN}$  is equal to the sum of all the energies supplied or spent on the moving structure.

Thus, as we know the numerical value of all these participants in the variation of this kinetic energy  $W_{CIN}$ , we can write equation Eq.31 which allows us to calculate  $W_{CIN}$  because all the terms of this equation are known.

$$W_{CIN} = (W_{DFCA1} + W_{BRIDGE1}) - (W_{DFCA2} + W_{BRIDGE2}) + W_{COULOMB} - (W_{CASIMIR1} - W_{CASIMIR2})$$

(Eq. 31) and fig 40.

All the terms of equation are known, so we know now the kinetic energy acquired by all the mobile system in  $z_1$  and know when the Coulomb force disappears in  $z_2$ . We know the intensity of  $W_{COULOMB}$  (Eq 27)

$$\text{All calculations done; we obtain: } W_{CIN} = \frac{1}{6} S \frac{\pi^2 \hbar c}{240} \left( \frac{1}{z_2^3} - \frac{1}{z_1^3} \right) + W_{COULOMB} \quad (\text{Eq .31}).$$

Let us calculate this final ascent position  $z_f$  of the mobile structure.

The Casimir force becomes a braking energy and will cancel this kinetic inertia plus that  $W_{DFCA2}$  stored in elastic energy.

After position  $z_2$ , the mobile structure has an inertia provided by the kinetic energy  $W_{CIN}$ , a stored elastic energy  $W_{DFCA2}$

The conservation of **energy** implies that the structure must now spend this inertia energy and reach a final position  $z_f$ .

$$\text{We know that } W_{CIN} = (W_{DFCA1} + W_{BRIDGE1}) - (W_{DFCA2} + W_{BRIDGE2}) + W_{COULOMB} - (W_{CASIMIR1} - W_{CASIMIR2}).$$

In order to obtain a correct but simpler order of magnitude of the stopping point  $z_f$  of the vibrating structure, we neglect the  $W_{BRIDGE}$  expression, so we then obtain the following:

$$W_{cin} = W_{DFCA1} - W_{DFCA2} + W_{COULOMB} - (W_{CASIMIR1} - W_{CASIMIR2}) \quad \text{We can calculate it with MATLAB .}$$

The sum of the kinetic energy of all the mobile parts (piezoelectric bridge plus mobile Casimir electrode), plus the energy memorized in the bride must be compensated by the breaking  $F_{CA}$  force.

We obtain

$$W_{CIN} + \frac{1}{6} S \frac{\pi^2 \hbar c}{240} \left( \frac{1}{z_2^3} - \frac{1}{z_f^3} \right) = \frac{1}{3} S \frac{\pi^2 \hbar c}{240} \left( \frac{1}{z_2^3} - \frac{1}{z_f^3} \right) \Rightarrow W_{CIN} = \frac{1}{6} S \frac{\pi^2 \hbar c}{240} \left( \frac{1}{z_2^3} - \frac{1}{z_f^3} \right)$$

We deduce of this equation that the final position  $z_f$  of the bridge is :  $z_f = \frac{1}{\sqrt[3]{\left[\frac{1}{z_0^3} - \frac{1440 W_{CIN}}{\pi^2 h c}\right]}}$  Eq 32.

We can see in Figure 35 that depending on the acquired inertia, which depends on the energy provided by the Coulomb force, the final return position  $z_f$  can slightly exceed its initial position  $z_0$ . We will use this property at the end of this article in order to increase usable energy.

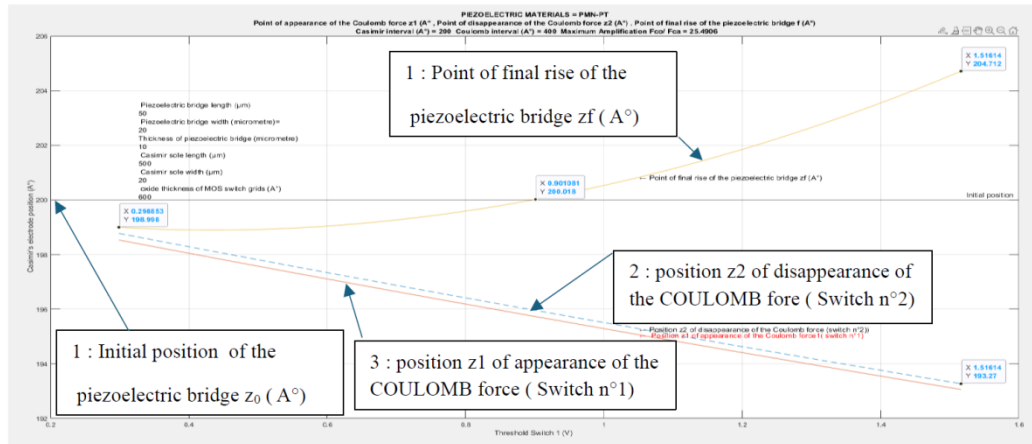


Fig 35: Positions of :1/ The final rise  $z_f$  of the structure, 2/ of the point  $z_2$  of disappearance of the Coulomb force depending on the threshold voltage  $V_{T2}$  of switch n°2, 3/ of the point  $z_1$  of appearance of the Coulomb force depending on the threshold voltage  $V_{T1}$  chosen for switch n°1

It is easy to calculate the damping energy  $W_{CASIMIR2}$  that appears between the intermediate position  $z_2$  and the final position  $z_f$ .

$$\text{We have } W_{CASIMIR2} = \int_{z_2}^{z_f} F_{CA} dz = \int_{z_2}^{z_f} S \frac{\pi^2 h c}{240 z_s^4} dz = S \left( \frac{\pi^2 h c}{720} \right) \left[ \frac{1}{z_f^3} - \frac{1}{z_2^3} \right] \quad (\text{Eq 33})$$

At position  $z_2$  the switch n° 2 commutes to ON and puts the Coulomb electrode to ground through the RLC circuit below (Fig 36) . The electrical charges present on the Coulombs electrode flow towards the ground, creating a current and a power which remains to be evaluated.

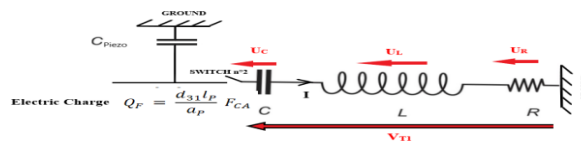


Fig 36 : RLC circuit to power the autonomous electronics for converting power peaks into direct voltage

We now evaluate this usable current flowing to ground. We put in the circuit, an adjustment capacitance  $C$  in series with  $C_{PIEZO}$ .

We call  $C$  the capacity of the capacities in series.

When the switch n°2 commutes, we have the equation :  $U_C + U_L + U_R = C_{PIEZO}/Q_F = V_{T1}$  ( fig 36) , with  $U_R = R I$ ,  $U_L = L dI/dt$  and  $Q_F = U_C C_{PIEZO}$ . With  $R$  resistance,  $L$  an inductance and  $C$  a capacity.

After rearranging we have the following equation  $\frac{d^2 U_C}{dt^2} + \frac{R}{L} \frac{dU_C}{dt} + \frac{U_C}{LC} = 0$  **Eq 33.**

This differential equation has solutions that depend on the value of its determinant  $\Delta =$

$$\sqrt{\left(\frac{R}{L}\right)^2 - \frac{4}{LC}}$$

We choose the values of R, L, C in such a way that the determinant  $\Delta$  of this equation is positive or vanishes.

So, if  $\Delta = 0$  the solution is :

$$x_1 = \frac{R}{2L} \left( -1 + \sqrt{1 - \frac{4L}{CR^2}} \right) = -\frac{R}{2L} \text{ and } x_2 = \frac{R}{2L} \left( -1 - \sqrt{1 - \frac{4L}{CR^2}} \right) = -\frac{R}{2L} \text{ then we have}$$

$$x_1 = x_2 = -\frac{R}{2L} < 0 \text{ Considering the initial conditions, we obtain}$$

$$u_c = \frac{V_{T1}}{x_1 - x_2} [x_1 \exp(x_2 t) - x_2 \exp(x_1 t)] \quad \text{Eq 34,}$$

$$i_c = C \frac{du_c}{dt} = C \frac{V_{T1} x_1 x_2}{x_1 - x_2} [\exp(x_2 t) - \exp(x_1 t)] \quad \text{Eq35}$$

The peak of current is given when  $d(i_c)/dt = 0$  so at the time  $t_{imax} = \frac{\ln\left(\frac{x_2}{x_1}\right)}{x_1 - x_2} = \frac{\ln\left(\frac{1 + \sqrt{1 - \frac{4L}{CR^2}}}{1 - \sqrt{1 - \frac{4L}{CR^2}}}\right)}{\frac{R}{L} \sqrt{1 - \frac{4L}{CR^2}}}$

**Eq 36**

Replacing t by  $t_{imax}$  in equations 34 and 35, we obtain the expression for the maximum of the voltage is  $u_{cmax} = V_{T1}$  and of the maximum current  $i_{cmax}$  ;

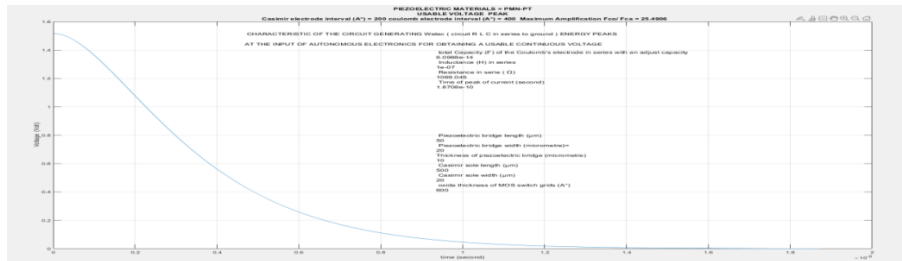


Fig 37 : Electric voltage on the capacitance C in series with the capacitance of the Coulomb electrode

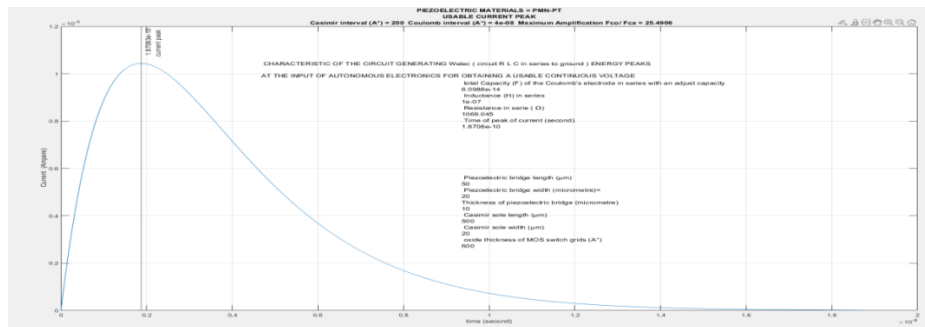


Fig 38 : The electric current flowing through the capacitance C in series with the capacitance of the Coulomb electrode



The electrical power of the signal is :

$$P(t) = u_c i_c = \left( \frac{V_{T1}}{x_1 - x_2} \right)^2 C x_1 x_2 [\exp(x_2 t) - \exp(x_1 t)] [x_1 \exp(x_2 t) - x_2 \exp(x_1 t)] \quad \text{Eq37}$$

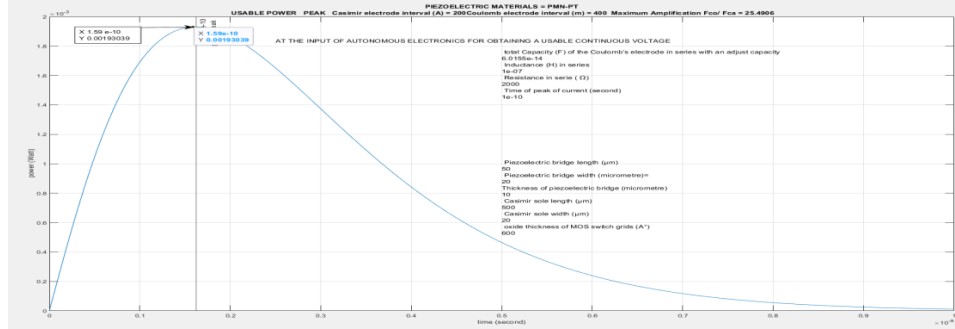


Fig 39: electrical power of the signal to power the autonomous electronics

We note on **fig 39** that the peak power of 1.93 mW is sufficient to power the autonomous electronics of fig 18,19 and obtain a useful voltage of several volts in a few milliseconds.( **fig 22**)The period of a vibration being (**fig 10**) of 0.2 μs for an F<sub>CO</sub>/F<sub>CA</sub> of simply 2, we calculate that the average power over a period is then approximately ≈ 0.3 μW.

We deduce that the total electrical energy provided by the system in 1 second is of the order of ≈ 0.3 μJ Knowing the electrical power P(time) , we can calculate the useful electrical energy

$$W_{ELECTRIC}(t) = \int_0^{10 \cdot t_{max}} u_c i_c dt = \left( \frac{V_{T1}}{x_1 - x_2} \right)^2 C x_1 x_2 \int_0^{10 \cdot t_{max}} [\exp(x_2 t) - \exp(x_1 t)] [x_1 \exp(x_2 t) - x_2 \exp(x_1 t)] dt \quad \text{Eq38}$$

We obtain W<sub>ELECTRIC</sub> in **fig 40**during one vibration of the MEMS

The energy balance is completed for the "RETURN " and we can now numerically evaluate this finale and useable energy, by MATLAB

$$\text{We have } W_{RETURNING} = W_{CIN} + W_{ELECTRIC} + W_{DFCA2} + W_{BRIDGE2} - W_{CASIMIR2} + \Delta Q_{vib}/2 \quad (\text{Eq 39})$$

In **Figure 40**, we can make the energy balance of the energies provided by the quantum vacuum in the "GOING" and "RETURNING" phases.

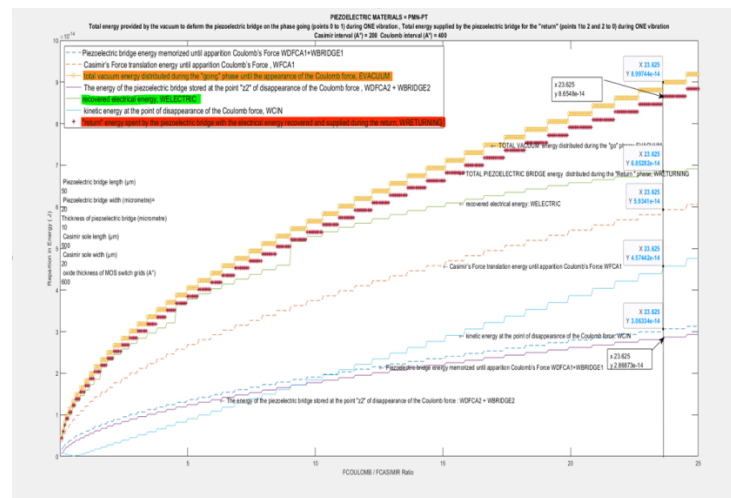


Fig 40: Balance of the energies of the "go" and "return" phases for the proposed MEMS which seems to be able to "extract energy from the quantum vacuum."

In the "GOING» phase , the total energy provided by the quantum vacuum ocean simply changes its nature and subdivides into other energies which are used in the "RETURN" phase of vibrations. One of these energies in this "RETURN" phase can be used by creating a **little electrical energy issue from the “nothing “** .

We note that the energy necessary for the perpetual maintenance of these vibrations is constantly provided by the isotropic and timeless energy of the quantum vacuum and that it is possible to extract from this gigantic ocean of energy of "nothing" a small electrical and exploitable energy. Whatever the  $F_{CO}/F_{CA}$  amplification factor, we note that  $W_{RETURNING}$  is always slightly lower than  $E_{VACUUM}$ , thanks to the choice of the coupling capacity  $C$  for the energy  $W_{ELECTRIC}$

We observed that in the referential of our 4 dimensions Space-Time plus the Quantic Vacuum, **the energy is conserved which is consistent with Noether's theorem**. This very important theorem of 1905 explains why, as Monsieur de Lavoisier said, "Nothing is created, nothing is lost, everything is transformed." .

Remember that energy is defined as the “physical quantity that is conserved during any transformation of an isolated system. However, the system constituted by simply the MEMS device in space is not an isolated system because a multitude of virtual particles is always created. While the system constituted by the MEMS device plus the space plus the energy vacuum seems an isolated system. The part of the MEMS energy sensor vibrates at frequencies depending on the size of the structure and operating conditions, but with amplitude of just a few Angstroms.

These vibrations are not a classical and impossible perpetual motion; because they can be continuously powered by the energy of the vacuum which brings among other things the translation energy of the Casimir force. WE DO NOT CREATE ENERGY FROM NOTHING, BUT "NOTHING" PROVIDES ENERGY.

The following diagram summarizes the operation of this presented MEMS ( Fig 41 and Fig 42 )

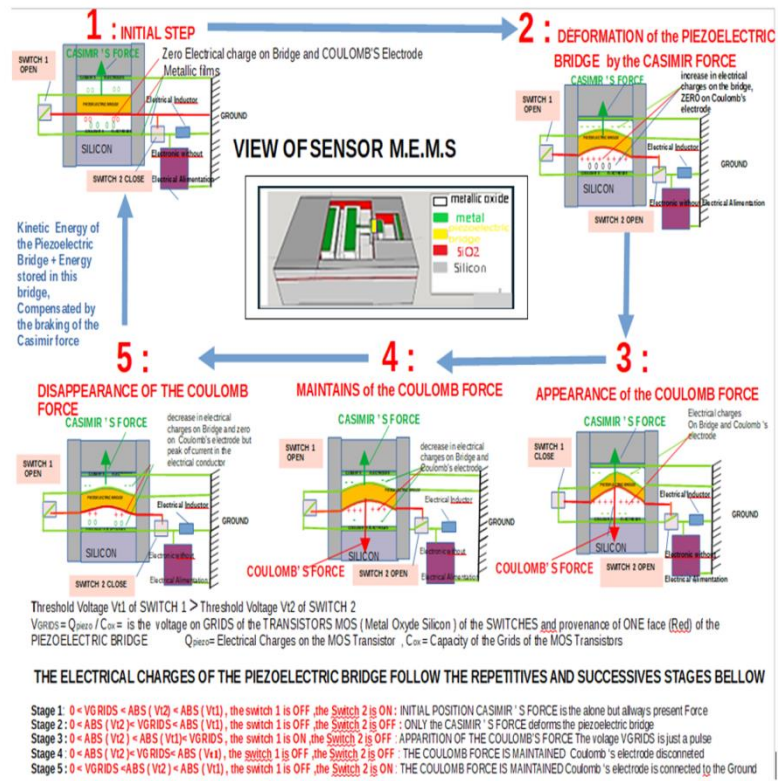


Fig 41: Overview of the 5 successive and repetitive steps of the M.E.M.S.

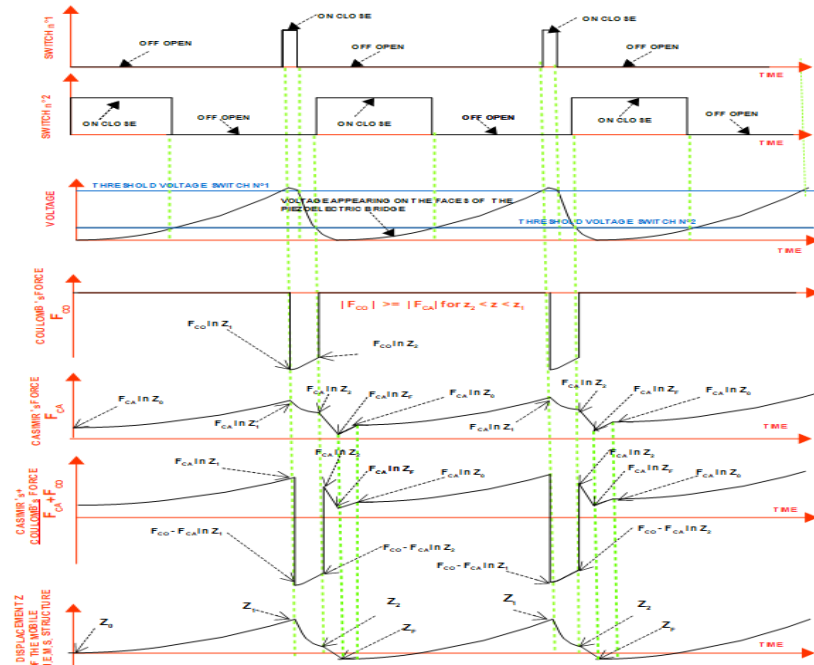


Fig 42: shape of the curves representing 1/ The switching of the two switches 2/ The electrical voltage on face 1 of the piezoelectric bridge 3/ The Casimir forces  $F_{CA}$  4/ The coulomb forces  $F_{CO}$  5/ the energies  $W_{FCO}$ ,  $W_{FCA}$ ,  $W_{FCO} - W_{FCA}$  6/ The maximum elevation  $z_f$  of the moving part

We notice in the previous pages that the piezoelectric bridge could reach a position  $z_f$  which exceeds its initial position  $z_0$ . We can take advantage of this observation by modifying the moving part of this MEMS to provide the RLC circuit with the two signs of current peak and voltage emitted by the sensor. This modification should increase the continuous electrical voltage on the capacitive output of the autonomous electronic circuit whose role is to transform the signals from the quantum vacuum energy sensor (fig 22)

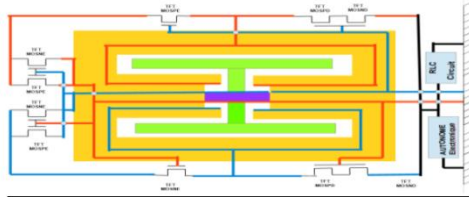


Fig 43: Shape of the MEMS circuit making it possible to double the direct voltage at the output of the autonomous electronic circuit, by providing it with consecutive voltage and current peaks of opposite sign.

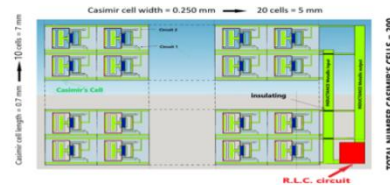


Figure 44: Positioning of 20 Casimir cells in parallel and 10 in series. Total of Casimir cells delivering a periodic current during a small part of the vibration frequency of the devices = 200. Total des cellules = 200,

In order to obtain an increase in current and voltage peak intensity, the Casimir cells can be positioned in a series and parallel network. A single RLC circuit as described above can be positioned at both terminals. For example, 20 Casimir cells can be placed in parallel and 10 in series, (Figure 44).

This work on the energy balance of a M.E.M.S., which appears to be able, theoretically, to extract energy from a new, totally unexploited source, was carried out completely alone and without the help of any organization, by an old retiree. It seems that - unless there is always a possible error - **the fundamental theorem of EMMY NOETHER from 1905 is not contradicted**. In the event of a theoretical confirmation by specialists, the supreme and definitive judgment will be the realization of a prototype, and I will be happy to participate in this development.

## 6. CONCLUSION

The theoretical results of this project seem sufficiently encouraging to justify the development of prototypes. If its theoretical predictions are confirmed, it will trigger a scientific, technical and human revolution, because the quantum vacuum can be used as a new source of energy both on Earth and in space with a considerable commercial market. As an inventor who has kept some details confidential, I would like to collaborate in its development after signing a contract with the potential investor

*"In the universe, everything is energy; everything is vibration, from the infinitely small to the infinitely large" Albert Einstein.*  
*"A person who has never made mistakes has never tried to innovate." Albert Einstein*

## REFERENCES

- [1] Fluctuations du vide quantique : Serge Reynaud Astrid Lambrecht (a), Marc Thierry Jaekel (b) a / Laboratoire Kastler Brossel UPMC case Jussieu F Paris Cedex 05, b / Laboratoire de Physique Théorique de l'ENS 24 rue Lhomond F 75231 Paris Cedex 05, Juin 2001
- [2] On the Attraction Between Two Perfectly Conducting Plates. H.B.G. Casimir, *Proc. Kon. Nederl. Akad. Wet.* 51 793 (1948)

- [3] Casimir force between metallic mirrors | Springer Link. E.M. Lifshitz, *Sov. Phys. JETP* 2 73 (1956); E.M. Lifshitz and L.P. Pitaevskii, *Landau and Lifshitz Course of Theoretical Physics: Statistical Physics Part 2* Ch VIII (Butterworth-Heinemann, 1980)
- [4] Direct measurement of the molecular attraction of solid bodies. 2. Method for measuring the gap. Results of experiments B.V. Deriagin( Moscow, Inst. Chem. Phys.), I.I. Abrikosova (Moscow, Inst. Chem. Phys.)Jul, 1956B.V. Deriagin and I.I. Abrikosova, *Soviet Physics JETP* 3 819 (1957)
- [5] Techniques de l'Ingénieur 14/12/2012 : l'expertise technique et scientifique de référence« Applications des éléments piézoélectriques en électronique de puissance » Dejan VASIC : *Maître de conférences à l'université de Cergy-Pontoise, Chercheur au laboratoire SATIE ENS Cachan*, François COSTA : Professeur à l'université de Paris Est Créteil, Chercheur au laboratoire SATIE ENS Cachan
- [6] 1. Wachel, J. C., and Bates, C. L., "Techniques for controlling piping vibration failures", ASME Paper, 76-Pet-18, 1976.
- [7] Jayalakshmi Parasuraman, Anand Summanwar, Frédéric Marty, Philippe Basset, Dan E. Angelescu, Tarik Bourouina «Deep reactive ion etching of sub-micrometre trenches with ultra-high aspect ratio Microelectronic Engineering» Volume 113, January 2014, Pages 35-39
- [8] F. Marty, L. Rousseau, B. Saadanya, B. Mercier, O. Français, Y. Mitab, T. Bourouina, «Advanced etching of silicon based on deep reactive ion etching for silicon high aspect ratio microstructures and three-dimensional micro- and nanostructure» *Microelectronics Journal* 36 (2005) 673–677.
- [9] Semiconductor Devices, Physics' and Technology S. M. SZE Distinguished Chair Professor College of Electrical and Computer Engineering National Chiao University Hsinchu Taiwan, M.K. LEE Professor Department of Electrical Engineering, Kaohsiung Taiwan
- [10] (M. BARTHES, M. Colas des Francs SOLID MECHANICAL VIBRATIONAL PHYSICS, ESTP: (Special School of Public Works)
- [11] Modélisation de transistors polysilicium en couches minces sur isolants : conception et réalisation d'écrans plats à cristaux liquides et matrices actives, Auteur Patrick Sangouard , These de doctorat Paris 11 , Soutenance en 1987, president du jury René Castagné <https://theses.fr/1987PA112461>